CHAPTER 1

INTRODUCTION

1.1 General

Economies of developed countries are generally influenced by rapid advances in energy system technologies. Electricity is a key input for fast economic growth of any nation. The transmission and distribution networks are important link between power generation and energy consumption/utilization. The technological sophistication presently available do not match the consumer's power quality and reliability demands effectively. Transmission and distribution congestion make a centralized grid inefficient and less reliable. In addition to this, there is an increasing risk for failure with increased peak demand. These factors, added to increased power consumption due to population growth further stretch the traditional grid to its limits, raising serious concerns on economic impact of blackouts and interruptions being seen today. While most recently (31st of July, 2012), the Indian grids failure has affected half of the country with millions hit by power cut caused by excessive power absorption, leading to massive snags in rail transport and medical facilities.

Smart energy devices leads to grid transformation which has provided the chance of enhancing efficiency of grid at reduced tariffs. It is also responsible for green i.e. clean power generation. In smart energy system, main concept is communication which entails basically digital information technology to be used in different applications to power system network optimization. Whereas, smart grid which is a common name heard today, is the application of such technology for generation, transmission and distribution of electricity through its various building blocks like efficient meters, intelligent control devices and most importantly a communication system that enables a consumer to provide excess energy back to the grid.

A distribution system is an interface between bulk power and custom powers, which maintains balance between two for the maintenance of continuous healthy operation of our system. The control of distribution system, usually means a system which is capable

to enhance system overall efficiency by considering features like loss reduction and power quality control. In recent years, some of the distribution side equipment's such as transformers, capacitor bank, synchronous machines, static volt-ampere reactive compensators (SVCs) and other compensating FACTS devices including DSTATCOM are applied for such controls. However, there are various challenges faced by the system with respect to smart-grid de-centralizing function which affect power system, such as voltage and reactive power compensation (now known as Volt-VAR optimization), power factor correction (PF), distribution system automation (DSA), phase current balancing, low loss transformers (for efficiency improvement), low loss transformers and some energy storage facilities (at consumer side).

For understanding power quality issues, we classify losses of distribution lines and transformers into resistive and reactive components. Among these losses, resistive losses cannot be avoided at any cost while reactive power losses which arises from capacitive and inductive circuit properties (should cancel each other) can be avoided. But the increase in demand of reactive power at the load side increases amount of current flowing through lines being responsible for energy losses. Distribution sides transformers often work at higher efficiency almost 97% as a result negligible core losses are produced. However, total losses of transmission and distribution system together constitute 9% of the total losses from generation to the consumer's end. Various academic groups in the world are presently doing research into control of DSTATCOM to remove power quality problems. In particular, with the evolution of current wave of smart grid, many multinational electricity companies are taking interest in DSTATCOM technologies with the hope of integrating such with the smart grid. These companies are Hitachi Europe, ABB, S & C Electric Company, GE, Schneider, and Siemens. Addressing the issues of Volt-VAR compensation & harmonic elimination aspect of solving the PQ problems at the distribution network is the theme of the present work.

1.2 Harmonics and Its Consequences

Harmonics in voltage or current of an electric power systems is generally as result of non-linear electric loads. Effect of harmonics in power systems is increased heating in the equipment and conductors, sometimes misfiring in variable speed drives, and lead to

torque pulsations in motors. Reduction of harmonics is considered essential for smooth and reliable operation of supply network.

1.2.1 Current Harmonics

In a normal alternating current (a.c.) power system, current is sinusoidal in nature at a specific frequency, in India it is 50 hertz. If a linear load is connected to the system, it always draws a sinusoidal current in phase or out of phase with the voltage, but has the same frequency as of voltage. Non-linear loads are responsible for current harmonics in the supply system. When a non-linear load, a converter (rectifier) is connected to the system, the current which is drawn by it need not to be of sinusoidal nature. Current waveform is solely depends on the type of load converter is feeding. To analyze this complex waveform, generally Fourier series analysis is used; it actually decomposes a non sinusoidal waveform into a series of simple sinusoids of different frequency components, i.e. fundamental & integer multiple of the fundamental frequency. Few more examples of non-linear loads are common office equipment's as Fluorescent lighting, computers and printers, variable-speed drives and battery chargers etc.

1.2.2 Voltage Harmonics

Cause of voltage harmonics are current harmonics. A non-linear load does not cause voltage harmonics if it is not injecting power. However, due to presence of source impedance, current harmonics distorts voltage source. Voltage harmonics introduced by current harmonics generally depends on the source impedance, as low as the source inductance lower will be the voltage harmonics.

1.2.3 Effect of Harmonics

Harmonics are generally a mathematical analysis of distortions in current or voltage waveform. According to Fourier series, it can be described as a periodic wave as sum of simple sinusoidal waves. A harmonics distortion is different from transient distortions as spikes, dips, etc. because they are steady state distortions which repeat itself after a period of time.

Basically harmonics are responsible for increase in current of the system, this is due to third harmonic which increases the magnitude of zero sequence components and in turn increases the current in neutral wire. This effect will require some special consideration in the design of an electric system to fulfill the need of non-linear loads without affecting other loads connected to the same supply system. Some other effects are a considerable reduction in voltage at the receiving end, because of voltage drop in the source reactance connected to the system.

Electric motor is one of the major devices use at the consumer's side. This device has some losses which depend on the frequency of supply. These losses are hysteresis loss and eddy current losses due to set up of eddy current in the iron core. Since frequencies of harmonics are higher than fundamental frequency, they produce higher core losses in a motor. Effect of this is increase in heating of core of motor, which might shorten the life of the motor. Along with other components, some components like 5^{th} harmonic cause a counter electromotive force (CEMF) in large motors, these acts in opposite direction of rotation. The CEMF does not change the basic nature and direction of rotation; however it affects the resulting rotating speed of the motor.

AC Voltage waveform generated by a generator is not a pure sinusoidal waveform, because it is generated by an ideal AC generator built with distributed stator and field windings which operates in a uniform magnetic field. In practical aspect, neither the magnetic field nor the winding distributions are uniform in an AC machine. As the voltage waveform distorts, voltage-time relationship will not remain pure sine function.

Actually, it seems that the effect of distortion is few percent of total but it exists. Because actual nature of voltage waveform is sinusoidal, deviation is periodic in nature and the voltage distortion contains harmonics.

1.2.4 Harmonic Disturbances

Harmonics are responsible for disturbances in electricity flow. This will deteriorate the power quality and causes a reduction in efficiency.

Main disadvantages of harmonics are:

(i) Increase in r.m.s current of distribution network,
(ii) Neutral current becomes more than phase current,
(iii) Increase in overload capacity of generator, transformer and motors along with that increase in transformer noise,
(iv) Overloading of shunt connected capacitors,
(v) Interference in telephone lines and communication network.

1.2.4.1 Economic aspect of disturbances

(i) Overloading of distribution network causes increased power loss, which increases equipment ratings and increased power level at consumer,
(ii) Reduction in life of equipments, they replaced sooner,
(iii) Unwanted halt of the supply due to unexpected tripping of protection devices.

1.3 Flexible AC transmission and custom power devices

Power flow control has traditionally relied on generator control, voltage regulation by means of tap-changing and phase-shifting transformers, and reactive power compensation using switched reactors and capacitors. Phase-shifting transformers have been used for the purpose of regulating active power in AC transmission network. In practice, some of them are permanently operated with fixed angles, but in most cases their variable tapping facilities are actually made use of. Series reactors are used to reduce power flow and series capacitors are used to shorten the electrical length of the lines, hence increasing the power flow. In general, series compensation is switched on and off according to load and voltage conditions. Until recently, these solutions served well the needs of electricity supply industry.

However, deregulation of the industry created the momentum for adopting new, radical technological development based on very high power solid-state electronic devices that promises to enhance the security, capacity and flexibility of power transmission systems

1.3.1 Classification of Flexible AC Transmission & Custom Power (FACTS) Devices

FACTS controller can be broadly divided into two groups:

(a) Line impedance and angle control (Series Compensation)

(b) Voltage control (Shunt Compensation)

First generation of FACTS controllers are:

(i) Static VAR Compensators (SVC)
(ii) Thyristor Controlled Series Compensation (TCSC)
(iii) Thyristor Controlled Voltage Regulator (TCVR)
(iv) Thyristor Controlled Phase Angle Regulator (TCPAR)

Second generation of FACTS controllers are:

(i) Static Synchronous Compensator (STATCOM)
(ii) Static Synchronous Series Compensator (SSSC)
(iii) Unified Power Flow Controller (UPFC)
(iv) Inter-Line Power Flow Controller (ILFC)

1.3.2 Benefits and applications of FACTS Controllers

A number of electrical utilities around the world have strategically been utilizing FACTS technologies for decades. Traditional reasons are:

(i) Provide better power flow control
(ii) Increase the transmission capacity
(iii) Improved voltage profile
(iv) Better utilization of existing transmission system assets
(v) Increased dynamic and transient grid stability
(vi) Increased quality of supply for sensitive industries

1.4 Implementation of FACTS controllers

Control strategy for active filters is implemented in three stages. In first stage, current and voltage signals are sensed using either instrumentation transformer or Hall Effect sensors to take system information. In second stage, various control methods are used to derive the amount of compensation of voltage or current signals using intelligent DSP control. In third and last stage gating signals for controlled switches are derived using pulse width modulation (PWM), hysteresis current controller (HCC) or fuzzy logic based control techniques. For designing of controlling part in real time various equipments like DSP, FPGA OR D-space can be used; earlier this work was achieved through complex analog and digital circuit.

1.4.1 Signal Conditioning

For implementing control algorithm instantaneous voltage and current signals are measured. These signals are used to evaluate various parameters like THD, power factor, crest factor, active and reactive power, etc. Voltage signals are supply voltage of phases and dc bus voltage. Current signal are load current, supply current and compensating current. Current and voltage signals have to be filtered to avoid any noise or interference problems. In hardware these filters are designed using analog circuit.

1.4.2 Compensating Current

Compensating signals can be of voltage signal or current signal. To draw compensating signals some control algorithm based on either frequency domain or time domain has to be designed.

i. **Frequency Domain Algorithm:** Fourier analysis is generally used to extract compensating in frequency domain. Switching frequency for device is kept twice of highest frequency component for accurate and effective compensation. Fourier transform has a disadvantage of producing large response time in the system.

ii. **Time Domain Algorithm:** Instantaneous values of compensation current or voltages are generally derived from polluted current or voltage signals.

In time domain large number of control methods has been derived as synchronous reference frame, instantaneous active and reactive power theory, etc.

iii. **Generation of Gating Signals:** General approaches for gating signal generation is based on PWM voltage or current method, hysteresis current control method, etc.

1.5 Objectives Of The Present Work

The main objectives of the present work are as follows;

i. To study different control algorithms for harmonic filtering such as Synchronous Reference Frame (SRF) theory, Anti-Hebbian (AH) Learning Algorithm, Character of Triangle Function (CTF) and Improved Linear Sinusoidal Tracer (ILST) based control algorithms and their application for the operation of distribution static compensator (DSTATCOM) through simulation study in MATLAB.

ii. Hardware realization of some advance control algorithm such as SRF, AH, CTF and ILST based control algorithms for the operation & control of DSTATCOM and assessment of their effectiveness under different operating conditions.

1.6 Outline of thesis

The chapter wise description of this dissertation is given as under:

Chapter-1 gives the introductory view of the overall work that has been presented in this thesis. This chapter also gives a brief introduction of FACTS devices and their use in series and shunt compensation.

Chapter-2 presents brief literature review of FACTS devices, D-STATCOM, control algorithm of D-STATCOM.

Chapter-3 discusses D-STATCOM modeling. In this chapter both Simulation and hardware based model of system is presented.

Chapter-4 presents the details of control algorithms and there designing approach used. This chapter also presents the implementation of control algorithms for operation of D-STATCOM in SIMULINK environment of MATLAB and hardware.

Chapter-5 presents the simulation and experimental results.

Chapter-6 gives the main conclusion and future scope of the work.

CHAPTER 2

LITERATURE REVIEW

2.1 General

As technology advances, its impact in both enhanced and degraded way is visible. Use of solid state devices enhanced the use of DC system in AC environment. But its effect in AC power quality can't be ignored on large scale. The emergence of power electronic loads in commercial and industrial application is a serious concern in the field of electric power engineering due to current/voltage distortion the loads. Power electronic devices with high rating as well as high switching frequency are most demanding in many power applications. Power-electronic devices are applied in electric power equipment, such as the uninterruptible power supply, switching power supply, arc furnace, AC/DC motor driver, trolley car, battery charger, and lighting appliances.

PQ problems are nothing but the deviation of voltage and current signals from there described nature. These deviations in technical terms are known as distortions. With advancement in technology, worldwide economy organizations have evolved towards globalization and the profit margins of many activities tend to decrease. Sensitivity towards vast majority of processes (industrial, services and even residential) to PQ problems turns the availability of electric power with quality a crucial factor for competitiveness in every activity sector. Due to disturbance, huge financial losses may happen, with the consequent loss of productivity and competitiveness. This all leads to design of compensation for harmonic and reactive currents as an important factor both for utilities and industries to feed their costly and sensitive equipment with quality power; thereby avoiding malfunction and loss of revenue. Shunt active power filters (SAPFs), also called active power line conditioners or active power quality conditioners, are best known tool for harmonic elimination as well as reactive power compensation, load balancing and voltage regulation. They are used as compensating current based technique in which load current harmonic filtering and reactive power compensation are employed. General configurations proposed by researchers are shunt, series, and hybrid and unified power quality conditioners.

Distribution Static Compensators (DSTATCOMs) based on voltage source converter (VSC) is a popular and effective active filter used to reduce the problems associated with AC distribution system. Performance of DSTATCOM depends on the estimation of active, reactive and harmonic currents. Control algorithm used for reference current generation decides the accuracy of DSTATCOM. From few decades, many control algorithms are reported in literature such as synchronous reference frame theory, instantaneous reactive power theory, and some Artificial intelligence based techniques. However, most of these attempts are either on other applications of these control algorithms or limited to simulation studies. In this section brief literatures review on static synchronous compensator is presented. In the last few decades about 25 books and more than 400 journal papers have been published in the area of power quality.

2.2 Distribution Static Compensator (D-STATCOM)

Narain G. Hingorani [1], described the basics of FACTS devices. It described all types of compensation devices which are connected in series, shunt or in both. It suggested that application of FACTS devices in all electrical energy areas. Power semiconductor devices offer high speed reliability of switches and variety in circuits enhances the value of electricity. This book provides basic depth in understanding FACTS devices. DSTATCOM basics are taken by this book along with the basic method of compensating techniques.

Arindham Ghosh [2], has described all the power quality related problems arise in existing power system. Main problem of power quality is due to the use of power electronics devices. It describes basics of harmonics and there effects in the existing power supply. This book also describes the basic principle of DSTATCOM and use of it in different modes along with the effect of PQ problems on grid and there effects.

H. Akagi et al. [3] explained basic theory of active filters (shunt and series). In this book, basic concept of control scheme is also discussed. Along with basic concept role of other controllers are also described.

Kalyan K Sen [4], in this paper describes theory and modeling technique of FACTS device STATCOM using electromagnetic transient program simulation. This paper explains

working of solid state VSI. This paper also verifies the function of STATCOM model by regulating reactive current flow through the tie line.

Dong Ju Lee et al. [5] described the simulation of STATCOM in this paper. Along with simulation part, this paper shows that STATCOM is better in continuous control of reactive power flow from other devices like SVC. This paper explains basic principle of STATCOM. It also verifies the basic operating characteristics by simulation.

Tariq Masood et al. [6] presented an analysis of STATCOM behavior against SVC controller. In this paper some operating parameters like stability, response time power losses and capability of real and reactive power exchange of STATCOM is compared with SVC. This paper concluded that STATCOM is more effective than SVC in improving transient stability.

Dong Shen et al. [7] analyzed performance of STATCOM under unbalanced and distorted system voltage. In this paper theoretical analysis of STATCOM is done by per-unit mathematical model under distorted system voltage. This paper showed algebraic expressions and 3-D curves to reveal relationship between harmonics and main circuit parameters.

S. H. Hosseini et al. [8] described STATCOM as a synchronous condenser. In this paper transmission capacity and transient stability of system is increased by STATCOM. For validation of STATCOM performance, a 230kV line for a two machine transmission system is used as a system.

Wang Chao et al. [9] used exact linearization method of non-linear control theory to linearize the non-linear state equations of STATCOM. In this paper, comparison of STATCOM operation under state feedback control and using general PI controller is compared.

M. Tavakoli Bina et al. [10] introduced average circuit model for STATCOM. This average circuit model produced mush faster simulation than produced by their exact models. This model is checked on both PSPICE and MATLAB environment to validate its performance.

Javid Akhtar et al. [11] presented actual status of active power filters based on power electronics devices. In this paper a brief description of PQ problems is given and role of active power filters for mitigation of PQ problems is defined. A comparison of active filters to that of conventional techniques is also discussed.

Boon Teck Ooi et al. [12] implemented a novel topology for STATCOM control operation. Advantage of this topology is direct voltage control by controlling gating pattern and reduction in dc bus capacitor. Order of dominant harmonics is also high, which can be filter easily.

Jianye Chen et al. [13] proposed a STATCOM where thyristor is used instead of self-commutated devices as switching device. This paper showed thyristor based VSC can absorb reactive power also by adjusting its firing angle.

Kamal Al-Haddad et al. [14] explained a comprehensive review on filters basically active filters, component selection, control strategies and other technical and economic considerations. This paper provides a detail review of the PQ issues and scope of prospective Active filters.

G. Casaravilla et al. [15] described possible methods of calculation when a selective shunt active filter is designed. This could be done by extraction of selective harmonic sequences based on modulation- filter- demodulation method. This method is generally based on p-q theory. To prove this method arc furnace current showing high harmonic content is used.

2.3 Synchronous Reference Frame (SRF) Theory

Bhim singh et al. [16] showed a comparative analysis of some basic algorithms. In this paper three methods instantaneous reactive power theory, synchronous reference frame theory and Adaline based algorithm are considered for analysis of DSTATCOM. This paper gives a detail simulation and hardware results.

D.M. Divan et al. [17] proposed a controller for hybrid series active filter based on SRF theory. In this paper, basic structure of SRF controller is discussed and its operation under

non-unity loop gain of controller is implemented. This paper also considered the design issues as well as effectiveness of active filter.

Vishal Verma et al. [18] showed a scheme which decomposes load current which is unbalanced in nature to balanced positive, negative and zero sequence components. This method is based on priority based scheme. This paper validated the simulation results in DSP based implementation of developed prototype.

G. C. Hsieh et al. [19] combined invention in PLL schemes with some IC technology. It contributed some improvement in performance and reliability of future communication systems. It provided higher accuracy and higher reliability servo control systems.

B. Widrow et al. [20] implemented a complete mean and mean square analysis of complex LMS algorithm for non-circular Gaussian signal. In this paper, analysis for conventional LMS and complex LMS algorithm is shown. Simulation results showed that complex LMS is better than conventional.

2.4 Anti-Hebbian Learning Algorithm

Sabha Raj Arya et al. [21] described a new neural network based control algorithm. In this control scheme Anti-Hebbian control algorithm is used, which is based on extraction of fundamental load components of active and reactive component in terms of weights. These weights are used to derive reference currents. Anti- Hebbian algorithm use least mean square (LMS) approach for error calculation.

S. Janpong et al. [22] presented a review on neural network application in SAPF. It shows three components like harmonic detection component, DC bus voltage control and compensating current based neural network technique. Objectives of papers are to increase efficiency, accuracy, robustness, etc.

Liu Kaipei et al. [23] showed a basic total least square estimation algorithm based harmonic detection. In this method for error detection TLS scheme is used, which estimate the error, then square it and reduces this by the use of filters.

Keqin Gao et al. [24] described an anti-hebbian learning scheme which is constrained. In this paper also TLS estimation is used and application of different filters like FIR and IIR is considered.

Qun Wang et al. [25] described an adaptive noise canceling technology (ANCT). This paper presents a neuron based adaptive detection approach. It also describes an analog circuit based realization scheme for the system.

Wang Xuhong et al. [26] presented a RBF neural network based controller. It predicts future harmonic current in the system. Optimization technique is used to produce values of control vector. Adaptive learning algorithm is used to make predictive model simpler and tighter. Space vector PWM technique is used to generate gating pulse of the inverter.

Abdelaziz Zouidi et al. [27] suggested a new control algorithm based on artificial neural network (ANN). In this paper a three layer ANN is used to analyze frequency same as FFT. Input for ANN is load current and target values are individual harmonic amplitudes which are calculated using FFT. These values are used to generate reference current.

Abdelaziz Zouidi et al. [28] presented an intelligent technique for harmonic detection. This method is based on again artificial intelligence technique named as ANN. In this paper focus is on adaptive linear neuron (ADALINE) for harmonic extraction.

Liu Chuanlin et al. [29] discussed harmonic detection based on least mean square (LMS). There is always a contradiction between steady state error and convergence rate. This paper proposes a new algorithm which controls dynamic detection of iteration process.

2.5 Character of Triangle Function (CTF)

Mohsen Mojiri et al. [30] presented an adaptive notch filter in this paper. This notch filter is able to achieve both Noise reduction and signal decomposition. This filter extracts a single sinusoid of time varying nature. For stability analysis of the system a local averaging theory is adopted. It provides instantaneous value of components and also adaptive to fundamental frequency, when compared with Fourier analysis.

Davood Yazdani et al**.** [31] introduced a new adaptive notch filter. It provides a synchronism between harmonic current and reactive current component for control strategy. This is applicable for uninterrupted power supplies, active power filters, etc for reference current generation.

Radu Iustin Bojoi et al. [32] presented an approach in which a renewable energy source is connected to the grid through inverter to control both active and reactive power flow to the supply. Control scheme adopted is the combination of sinusoidal signal integrator for reference current generator and IRP theory with current controller.

Zhihua Bao et al. [33] showed a deadbeat control which is based on coherent average. It suppresses the effect of noise on compensation performance, improve accuracy and ensure fast dynamic response. This method is checked on simulation and results shows the method proposed could predict the command current more accurately with frequent load current change and also in low signal-to-noise ratio.

Sabha Raj Arya et al. [34] described that CTF is a pure mathematics based algorithm, which can be designed by using some multipliers and filters. As components requirement of this algorithm is very less so it is fast in terms of reaching steady state condition. In this approach transient time is very less so it is stable in terms of frequent change in load conditions and in the occurrence of sudden disturbance.

S. Ali Khajehoddin et al. [35] presented a method to connect a renewable energy source to grid through an output type filter. Type filter is used to filter out coupling terms. Feedback controllers are used to get robustness with grid frequency. This paper also presents a new controller to improve transients of the system. Feedback linearization methodology is used in this paper.

2.6 Improved Linear Sinusoidal Tracer (ILST)

Bhim Singh et al. [36] described an improved version of Linear Sinusoidal Tracer (LST) for mitigation of PQ problems. In LST error between reference value and actual value is affected by some higher order harmonics. So this algorithm does not detect harmonic

current with accuracy. In ILST a low pass filter is used to filter out these harmonics and along with that both source and reference current trace each other.

Ambrish Chandra et al. [37] presented the Linear Sinusoidal Tracer (LST) algorithm. For extraction of three-phase fundamental load active power component of current, zero crossing detector (ZCD) is used as a trigger pulse of sample and hold (SHC) circuit. These components are easy to handle and their impact on system does not lead to any kind of irregularity.

Vincent George et al. [38] presented a detailed study on user defined constant switching (UDCS) frequency DSTATCOM. In VSI out of four legs, three are operated in hysteresis current tracking mode and fourth leg by a user defined square switching pulse.

Shailendra Sharma et al. [39] suggested a voltage and frequency controller (VFC). In this method indirect current control of VSC is employed which uses single phase PQ theory to control voltage and frequency. For implementation, a transformer is used. This transformer provides a neutral for four wire load, this will compensate neutral current. Reduction in neutral current reduces the rating of VSC.

Yi Fei Wang et al. [40] described a method based on cancellation of delay. Frequency domain control generally provides one cycle of time delay and time domain methods uses complex filtering techniques. In this method anti-conjugate harmonic decomposition is used. This approach is simple and robust.

2.7 Conclusion

This literature review provides a basic knowledge in the area of PQ. It provides a knowledge about types of control algorithms already implemented in past, there advantages, disadvantages, etc. this review provides a knowledge about what are those parameters which can be controlled to provide better performance of the system. A SRF theory introduces a time delay in the circuit, so there is a chance of flow of high amplitude current, whenever this algorithm is implemented in hardware. Other methods which are new in these fields are artificial intelligence based algorithms. These algorithms are ruling over other algorithms in terms of efficiency, accuracy, performance, etc. Algorithms based on soft computing techniques show better performance than conventional algorithms. Some

conventional algorithms like CTF is good in terms of simplicity because it uses only multipliers, summers, etc. Anti- hebbian like neural network techniques works better in condition of dynamic changes in the loads.

CHAPTER 3
MATHEMATICAL MODELLING & CONTROL OF DSTATCOM

3.1 General

In this chapter modeling and control of the shunt compensation device have been presented in detail. Model of voltage source converter and its control scheme is essential for simulation study and design of PQ compensating devices for a particular application.

3.2 Description of shunt controller

The system under consideration is shown in Fig 3.1.The nonlinear load injects harmonics in the supply system, the DSTATCOM which acts as a shunt current controller injects the different current in the system without changing the load current.

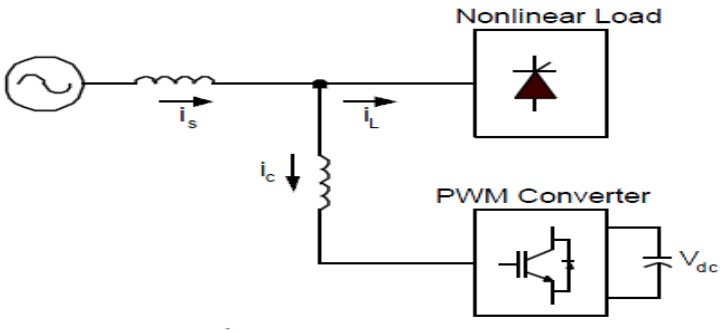

Fig 3.1 Basic Structure of DSTATCOM

Fig 3.2 shows schematic diagram of a DSTATCOM system supporting the reactive power and harmonic current to power electronics based non-linear load. This system shows a balanced three phase supply connected to a balanced three phase load. The source resistance (R_s) and inductance (L_s) are included in model equation to represent the characteristics of distorted system. Source resistance is generally low in stiff supply system. The source, load and VSC are connected together and their interfacing point is referred as point of common coupling (PCC).

There are two types of load shown in this diagram, one is linear and other is non- linear. Our concern is non -linear loads; because they draw reactive power along with that they are responsible to impart some non- linearity in the system. Linear loads draws only fundamental component of current, whether they are connected to pure supply or polluted supply.

Main aim of control scheme is to generate reference source current which get compared with the actual source current and error between both will generate gate signal for DSTATCOM.

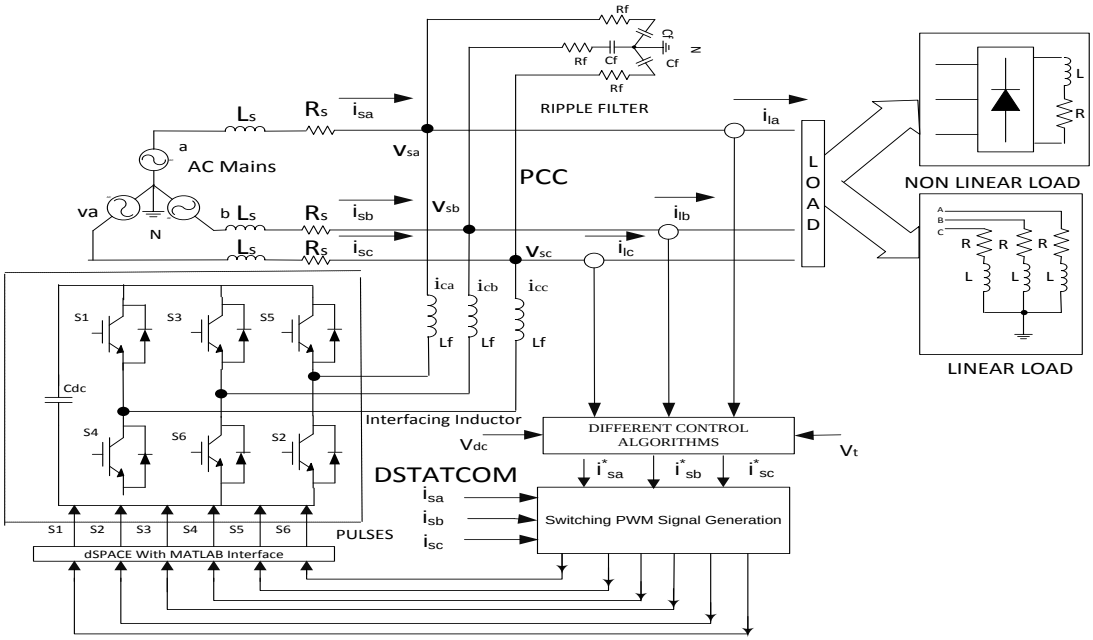

Fig 3.2 A schematic diagram of a DSTATCOM for reactive power compensation and harmonic elimination in non-linear load

DSTATCOM is a VSC with capacitor at dc side. If battery is connected at the dc side then it can supply only active power but when capacitor is connected, it will supply or absorb reactive power. To operate VSC, there is a need of six gating pulses for its power switch i.e. IGBT, these pulses can be obtained by either pulse width modulation (PWM) or hysteresis current controller (HCC). The HCC provides good response by reducing some of

high order disturbances but it makes speed of the system slow. A HCC is easily implemented in software but its implementation using dSPACE causes time delay. The rating and values of various parameters are given in the Appendix.

3.3 Mathematical modeling of DSTATCOM

Fig 3.3 shows the equivalent circuit of DSTATCOM which is connected to a distribution system through filter inductors. In Fig.3.3 v_a, v_b, v_c represent the three phase line-to-neutral system voltages at PCC. e_a, e_b, e_c, represent the fundamental three phase line-to-neutral output voltage of the DSTATCOM's converter. The resistance (R_f) and inductance (L_f) represents reactance of interfacing inductors. R_p accounts for losses in converter devices. i_a, i_b, i_c represents line currents flowing through VSC. C_{dc} is capacitance on DC side of converter.

From Fig.3.3 KVL equations at PCC can be written as

$$e_a = i_a R_f + L_f \frac{di_a}{dt} + v_a \tag{3.1}$$

$$e_b = i_b R_f + L_f \frac{di_b}{dt} + v_b \tag{3.2}$$

$$e_c = i_c R_f + L_f \frac{di_c}{dt} + v_c \tag{3.3}$$

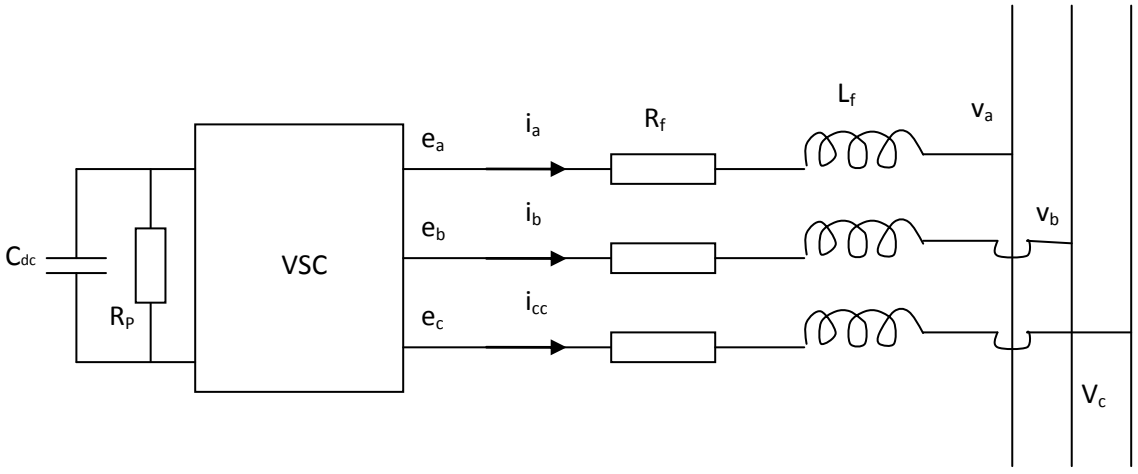

Fig 3.3 Equivalent circuit of DSTATCOM

In matrix form these equations can be written as

$$\frac{d}{dt}\begin{bmatrix} i_a \\ i_b \\ i_c \end{bmatrix} = \begin{bmatrix} \frac{-R_f}{L_f} & 0 & 0 \\ 0 & \frac{-R_f}{L_f} & 0 \\ 0 & 0 & \frac{-R_f}{L_f} \end{bmatrix} \begin{bmatrix} i_a \\ i_b \\ i_c \end{bmatrix} + \frac{1}{L_f}\begin{bmatrix} e_a - v_a \\ e_b - v_b \\ e_c - v_c \end{bmatrix} \tag{3.4}$$

If $\frac{d}{dt}$ is represented as p, then above eq. (3.4) becomes

$$p\begin{bmatrix} i_a \\ i_b \\ i_c \end{bmatrix} = \begin{bmatrix} \frac{-R_f}{L_f} & 0 & 0 \\ 0 & \frac{-R_f}{L_f} & 0 \\ 0 & 0 & \frac{-R_f}{L_f} \end{bmatrix} \begin{bmatrix} i_a \\ i_b \\ i_c \end{bmatrix} + \frac{1}{L_f}\begin{bmatrix} e_a - v_a \\ e_b - v_b \\ e_c - v_c \end{bmatrix} \tag{3.5}$$

Converting a-b-c to d-q quantities using Parks transformation using eqn. (3.6), we can write

$$\begin{bmatrix} i_d \\ i_q \\ i_0 \end{bmatrix} = \frac{2}{3}\begin{bmatrix} Cos\theta & Cos\,(\theta - \frac{2\pi}{3}) & Cos\,(\theta + \frac{2\pi}{3}) \\ -Sin\theta & -Sin\,(\theta - \frac{2\pi}{3}) & -Sin\,(\theta + \frac{2\pi}{3}) \\ \frac{1}{2} & \frac{1}{2} & \frac{1}{2} \end{bmatrix} \begin{bmatrix} i_a \\ i_b \\ i_c \end{bmatrix} \tag{3.6}$$

Where i_d, $i_q$and i_0 are direct, quadrature and zero sequence component of current. Zero sequence component remains zero for three phase- three wire balanced system. θ is transformation angle.

Using eq. (3.6), eq. 3.5 can be written as

$$p\begin{bmatrix} i_d \\ i_q \end{bmatrix} = \begin{bmatrix} \frac{-R_f}{L_f} & \omega \\ -\omega & \frac{-R_f}{L_f} \end{bmatrix} \begin{bmatrix} i_d \\ i_q \end{bmatrix} + \frac{1}{L_f}\begin{bmatrix} e_d - v_d \\ e_q - v_q \end{bmatrix} \tag{3.7}$$

Where, $\omega = \frac{d\theta}{dt}$

Equation (3.7) may be written in the following form:

$$p\begin{bmatrix} i_d \\ i_q \end{bmatrix} = \begin{bmatrix} \frac{-R_f}{L_f} & \omega \\ -\omega & \frac{-R_f}{L_f} \end{bmatrix}\begin{bmatrix} i_d \\ i_q \end{bmatrix} + \begin{bmatrix} 0 & \omega \\ -\omega & 0 \end{bmatrix}\begin{bmatrix} i_d \\ i_q \end{bmatrix} + \begin{bmatrix} x_1 \\ x_2 \end{bmatrix} \quad (3.8)$$

Where $x_1 = \frac{1}{L_f}(e_d - v_d)$ (3.9)

$$x_2 = -\frac{1}{L_f}(e_q) \quad (3.10)$$

Assuming d-axis coincides with the voltage vector, v_q becomes zero.

Neglecting the Voltage harmonics produced by the inverter, we can write the pair of equation for e_d and e_q

$$e_d = k v_{dc} \cos\alpha \quad (3.11)$$

$$e_q = k v_{dc} \sin\alpha \quad (3.12)$$

where k is a factor for the inverter which relates the DC-side voltage to the amplitude (peak) of the phase–to-neutral voltage at the inverter AC-side terminals, v_{dc} is dc side voltage and α is the angle by which the inverter voltage leads the line voltage vector.

3.4 Designing of PI controllers

To design PI-controllers, (AC voltage regulator and DC link voltage regulator) following factors must be considered while dealing with Hit-and-trail method. It is desirable that the control system be under-damped from the point of view of quick response. An under-damped control system exhibits exponentially decaying oscillations in the output during the transient period. For satisfactory performance of a control system a convenient adjustment has to be made between maximum overshoot and steady state error. The proportional control action tends to stabilize the system while the integral control action tends to eliminate or reduce steady-state error in the response to various inputs. Integral control action while removing offset or steady-state error, may lead to oscillatory response of slowly decreasing amplitude or even increasing amplitude, both of which are undesirable. Except for certain applications where oscillations can't be tolerated, it is desirable that the transient response be sufficiently fast and damped. Both the maximum

overshoot and the rise time can't be made smaller simultaneously. If one of them is made smaller, the other increases. The gain constant K_I controls the rate of integration and thus the speed of response. The block diagram of PI controllers is shown in Fig.3.4.

Fig 3.4 shows a block diagram of PI controller for regulating AC voltage. The peak amplitude of AC side phase voltage ($\mathbf{V_m}$) is estimated using sensed three-phase supply voltage.

3.4.1 AC Voltage Regulator

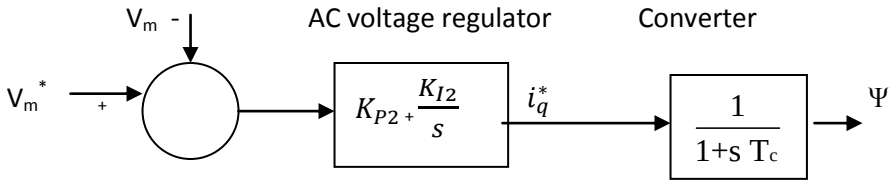

Fig. 3.4 AC voltage regulator

The peak amplitude of AC voltage is compared with the reference AC voltage ($\boldsymbol{V_m^*}$) and error is processed by PI controller. The constants $\boldsymbol{K_{P2}}$ and $\boldsymbol{K_{I2}}$ are adjusted suitably to determine the magnitude of needed reactive power component of compensating current ($\boldsymbol{i_q^*}$). Primary function of D-STATCOM is to regulate ac bus voltage to which it is connected. AC voltage regulator regulates the ac bus voltage by modulating the magnitude of the STATCOM bus voltage by varying the modulation index $\boldsymbol{m_a}$ of the converter.

3.4.2 DC Voltage Regulator

Fig 3.5 shows transfer function of DC voltage regulator. DC voltage regulator is a PI controller which maintains DC bus voltage constant after any disturbance. K_{P1} and K_{I1} are the proportional and integral gain settings of the DC voltage regulator $V_{dc.}$

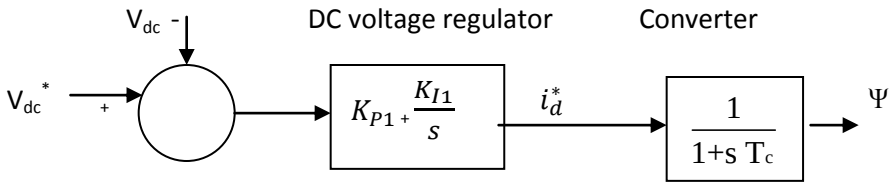

Fig 3.5 DC voltage regulator

3.5 Hardware description

The prototype model of DSTATCOM is designed and developed for regulating AC side voltage of 240V.The necessary control signals are generated by sensing AC and DC side voltage of DSTATCOM.

3.5.1 Hall Effect Sensor

A sensor is a converter that measures a physical quantity and converts it into a signal. LEM voltage & ABB current sensors are being used in the project. A current sensor is a device that detects electrical current (AC or DC) in a wire, and generates a signal proportional to it. The generated signal could be analog voltage or current or even digital output. It can be then utilized to display the measured current or can be stored for further analysis in a data acquisition system. The voltage sensor is used to sense the voltage from three-phase supply voltage. ABB current sensors are based on Hall Effect technology. They allow for the measurement of direct, alternating and impulse currents, with galvanic insulation between the primary & secondary circuits.

The electronic circuit amplifies this voltage and converts it into secondary current which multiplied by the number of turns of secondary winding cancels out the primary magnetic flux.

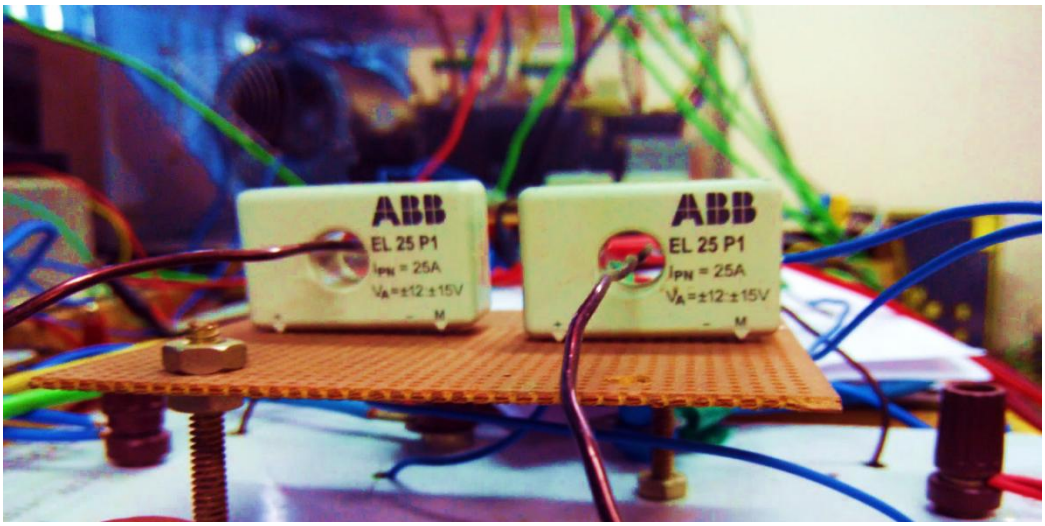

Fig 3.6 Current Sensors

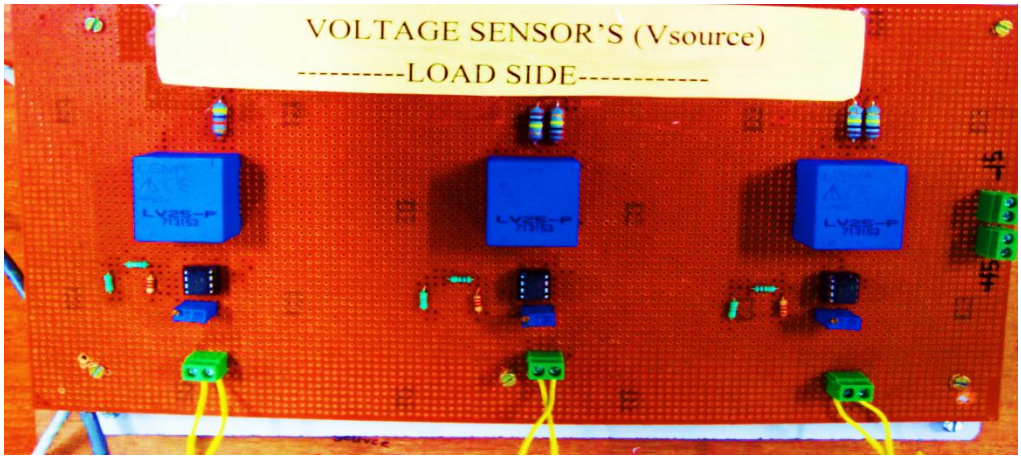

Fig 3.7 Voltage Sensors

The current sensor is used to sense the current in any two phases and the third current is estimated using these two currents.

(i) The LEM voltage sensor used is in the project is LV 25-P (700V).

(ii) The ABB current sensors used are ABB25-P (25A).

These currents and voltage values are input to dSPACE system. Output of these sensors are small amount of current, so a resistance in put in series to the sensor and voltage drop across it is taken as the input to dSPACE.

3.5.2 Non-linear Load

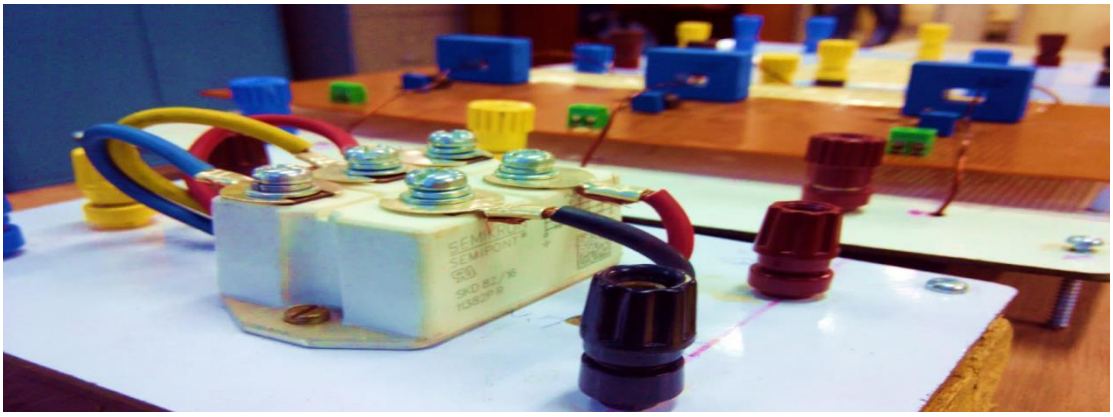

Fig 3.8 Rectifier Module

Three phase diode rectifier module (ABB) with R-L load is being connected as three-phase non-linear load. This load draws harmonic current from AC supply.

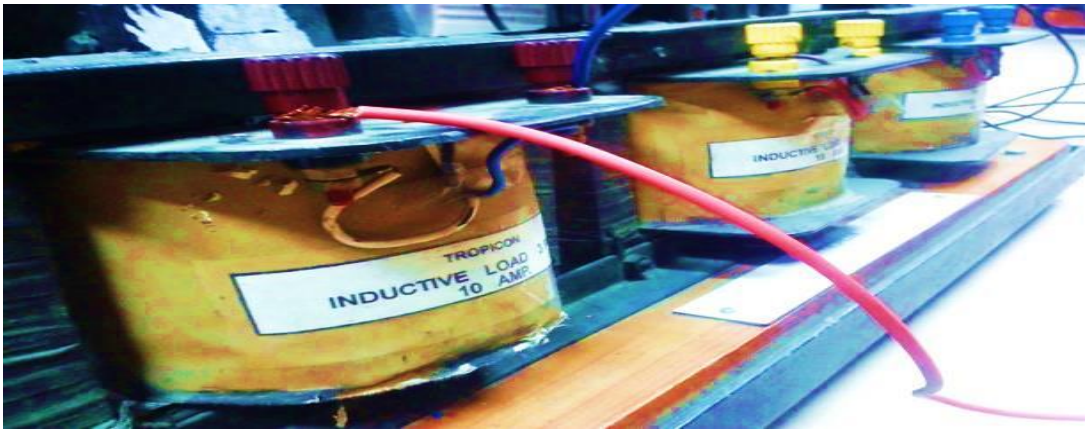

Fig 3.9 Inductive load

3.5.3 DS1104 Control Board

The DS1104 R&D Controller Board upgrades the PC to a development system for rapid control prototyping (RCP). The real-time hardware, based on a PowerPC microprocessor and its I/O interfaces make the board ideally suited for developing controllers in various fields, in both industry and academics. The DS1104 R&D Controller Board is a standard board that can be plugged into a PCI (Peripheral Component Interconnect) slot of a PC. The DS1104 is specifically designed for the development of high-speed multivariable digital controllers and real-time simulations in various fields. It is a complete real-time control system based on a 603 PowerPC floating point processor running at 250 MHz. For advanced I/O purposes, the board includes a slave-DSP subsystem based on the TMS320F240 DSP microcontroller. Interfacing of DS1104 & PC-MATLAB is done in order to ease the operation of control [50]. The three-phase current and speed once sensed are fed to the ADC port of DS1104 by means of BNC cable. DS1104 interfaces with the MATLAB, where the control circuit is designed. The gate pulses are determined through the control circuitry. These gate pulses are then fed to the inverter through the Digital I/O connector port of DS1104 separated by the isolating circuit in order to prevent the gate from being shorted [51]. The pulses determine the amount of reactive power supplied by DSTATCOM.

The DS1104 contains two different types of analog/digital converters (ADCs) for the analog input channels,

(i) One 16-bit ADC with four multiplexed input signals: the channels, ADCH1 ... ADCH4
(ii) Four 12-bit parallel ADCs with one input signal each: the channels, ADCH5 ... ADCH8

The digital I/O connector (CP17) is a 37-pin, male Sub-D connector located on the front of the connector panel. The important thing to note is that the ADC input to the DS-1104 should be between ±10 V. In order to make this possible, the gain of current sensor and voltage sensor are accordingly set in the circuit. Fig 3.10 shows control desk screen of dSPACE. This is also known as CRO of dSPACE [52].

Fig 3.10 dSPACE Control Desk screen

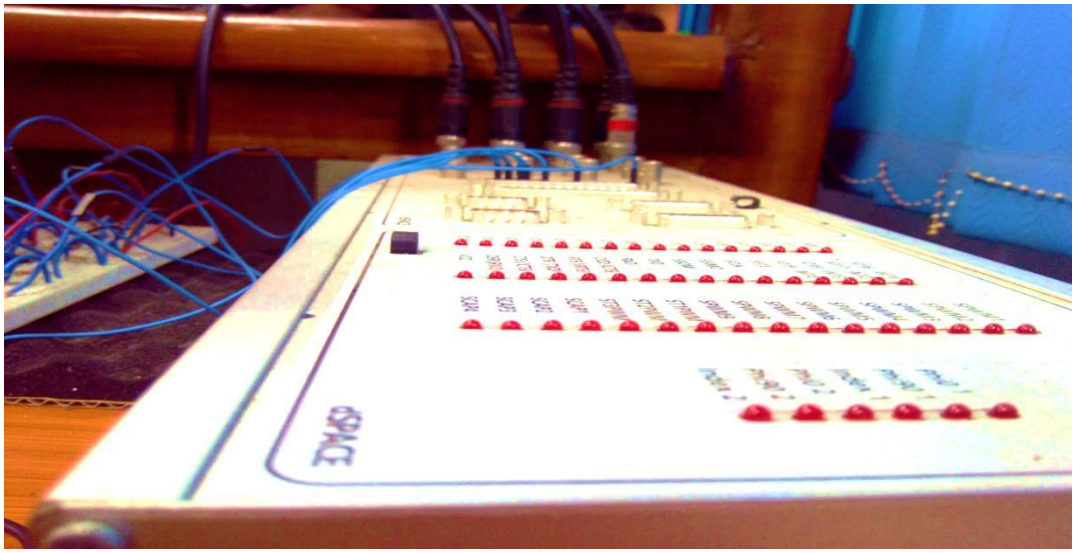

Fig 3.11 dSPACE DS-1104

In this CRO system parameters like supply voltage, current, firing pulses, etc. can be viewed both in waveform pattern as well as in magnitude.

3.5.4 Voltage Source Converter

A converter is a term coined in general for a rectifier or an inverter. A rectifier converts AC voltage into DC voltage while as an inverter converts DC voltage into AC voltage. A three phase Voltage Source Inverter (VSI) is used in the hardware implementation of the scheme, manufactured by the Semikron Industries (shown in Fig 3.12). The Voltage source converter consists of a three phase diode bridge rectifier which converts AC voltage into DC voltage and the VSI consists of three phase IGBT bridge inverter. The VSC consists of capacitors to filter the DC link voltage. In the VSI, IGBT semiconductor switches are used. The IGBT is suitable for many applications in power electronics, especially in Pulse Width Modulated (PWM) servo and three-phase drives requiring high dynamic range control and low noise. IGBT improves dynamic performance and efficiency and reduces the level of audible noise. It is equally suitable in resonant-mode converter circuits. Optimized IGBT is available for both low conduction loss and low switching loss. It has a very low on-state voltage drop. It can be easily controlled in high voltage and high current applications. A block diagram showing the IGBT based VSC is shown in Fig. 3.12.

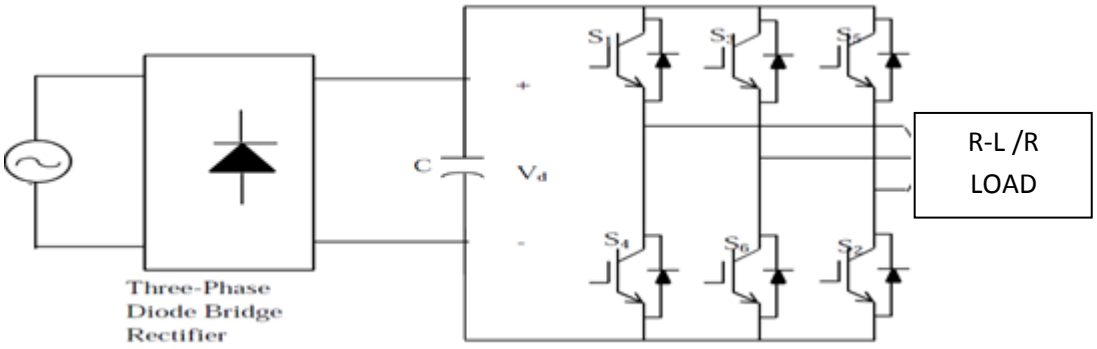

Fig 3.12 Voltage Source Converter (IGBT Based)

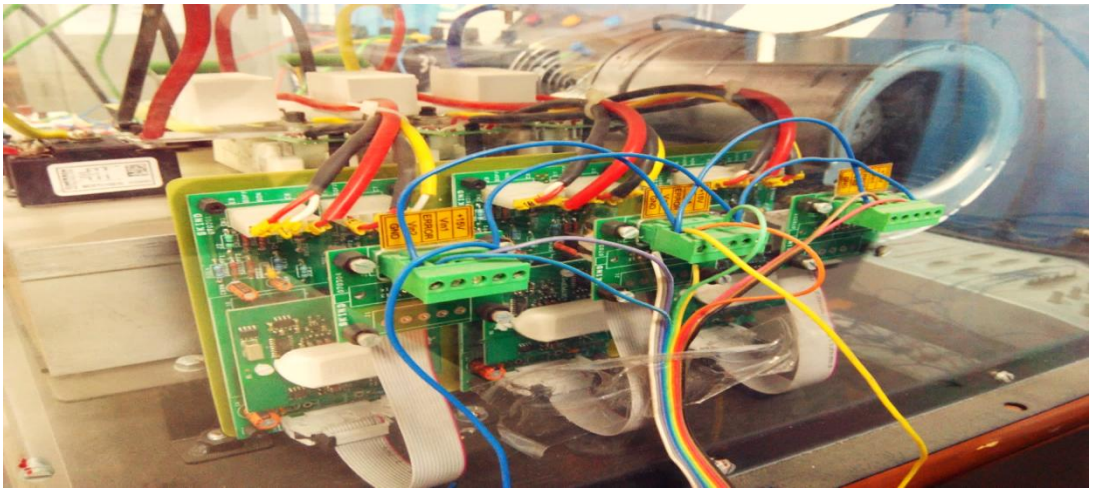

Fig 3.13 SEMIKRON B64U VSC

The rectifier circuit works in the ratio of 1:1.35 i.e. for an input ac line voltage of 100 V, the rectifier output is a 135 V dc voltage. The pulses to the inverter are PWM pulses generated from the MATLAB model using a Hysteresis current controller and fed to the inverter through DS-1104 isolated using an opto-coupler circuit.

3.5.5 Interfacing Inductors

For interfacing VSC with actual supply line, filter inductors (shown in Fig 3.13) of value 2.3mH are used.

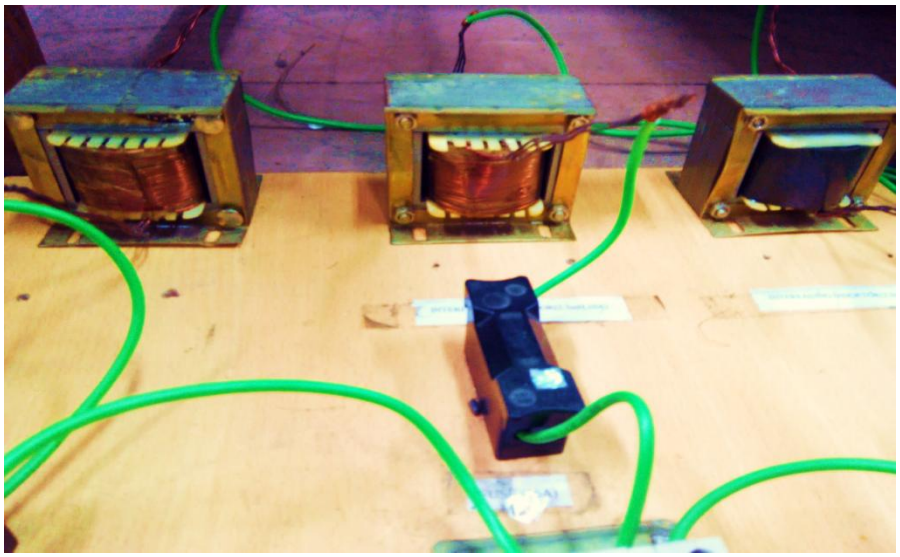

Fig 3.14 Interfacing filter Inductors

These inductors will limit the amount of circulating current flowing through the circuit in case of difference in phase between actual power supply and that of inverter supply we are going to connect. Some mathematical calculations are done to determine the number of turns, number of core plates, width of gap, etc. for inductor design. By changing the width of gap between E & I core, value of inductance can be changed [47- 49]. Ratings of these inductors are 2.5mH, 15A. For safety purpose fuse of value 10A and MCB of 15A is used.

3.5.6 Gain Circuit

Firing pulses generated by dSPACE is of 5V amplitude. The VSC switches are triggered at the voltage of 15V, for increasing voltage level and to provide isolation gain circuit is designed. This gate driver circuit is made by opto-coupler (6N139) and CE amplifier using 2N222 transistor shown in Fig 3.15.

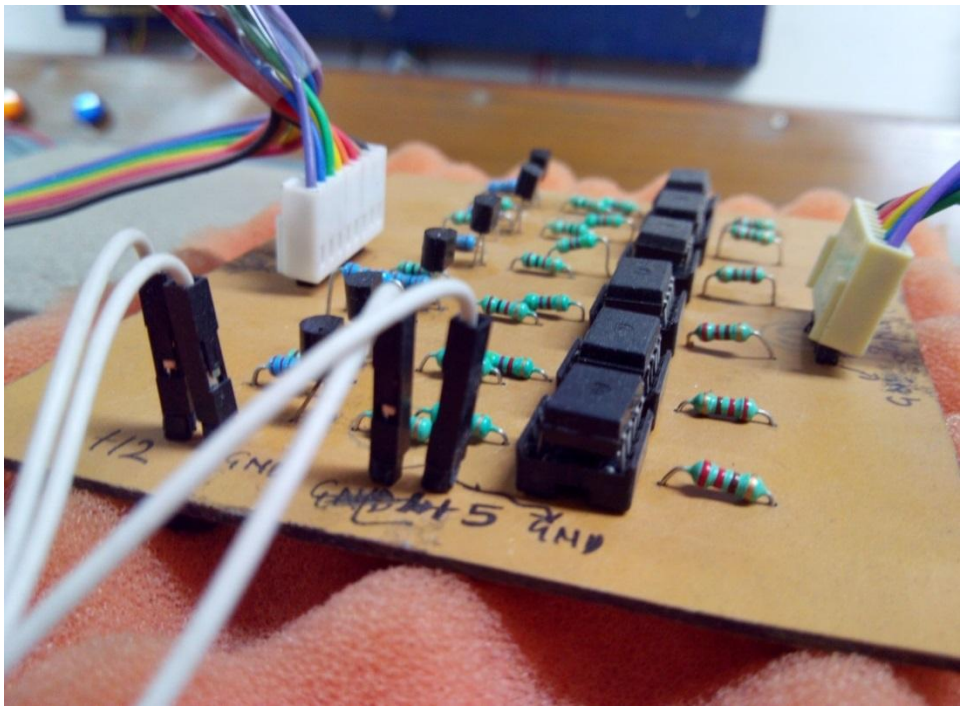

Fig 3.15 Opto-coupler (6N139) and Gain Circuit

3.6 Overview of Experimental setup

Fig 3.15 shows complete experimental setup. It consists of current and voltage sensors with voltage source converter and all the components described above.

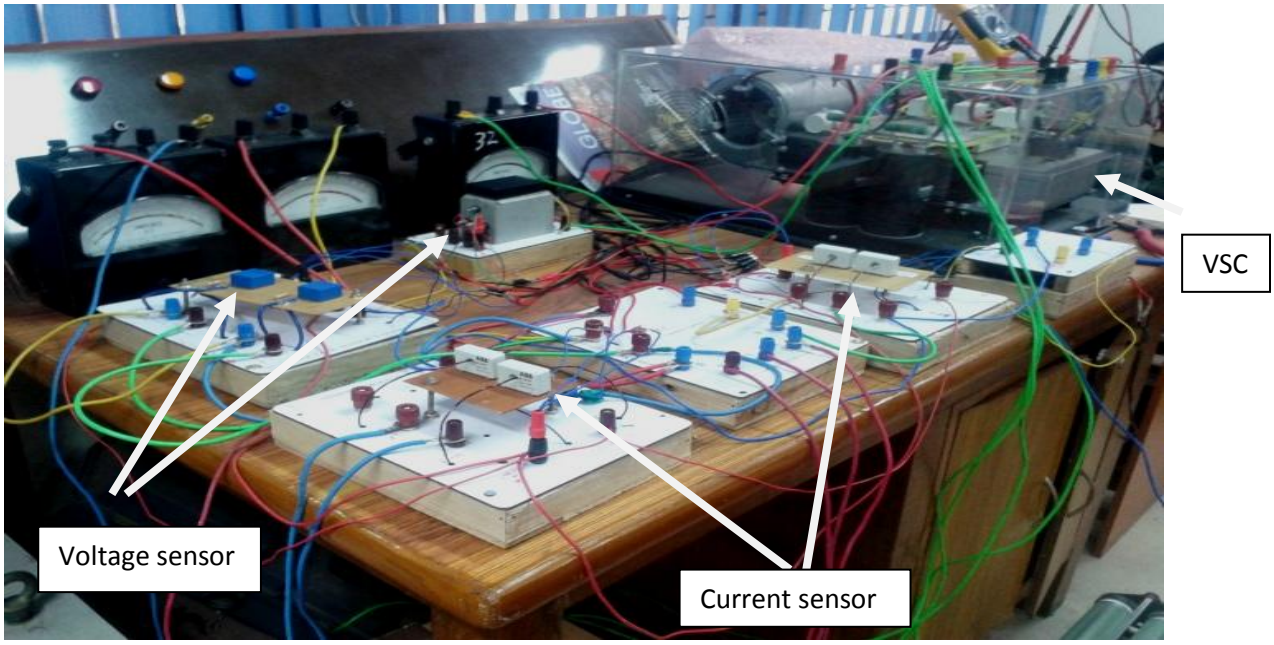

Fig 3.16 Overview of experimental setup

3.7 Conclusion

This chapter explains mathematical modeling and hardware setup of the system. In this chapter devices used for experimental setup of the system is discussed. For real time implementation of the system, many devices are required like sensors, VSC, inductors, etc. for interfacing control algorithm to real time dSPACE is used as interfacing device. In dSPACE inputs are three-phase supply voltage and current (both source and load) and output is firing pulses for VSC.

CHAPTER 4

MATHEMATICAL DESCRIPTION OF CONTROL ALGORITHMS USED FOR OPERATION OF DSTATCOM

4.1 General

DSTATCOM performance depends on control algorithms used for generation of reference current. Many control algorithms based on mathematical approach and soft computing techniques like neuro-fuzzy control algorithm, etc. are reported in literature. Main application of control algorithms is to estimate reference current. Nowadays artificial intelligence based techniques mainly neural network based techniques are used in large scale. In this chapter few control algorithms based on different approaches are explained.

4.2 Classification of control algorithms

Objective of control scheme is to extract fundamental component of current from polluted current signal. In this dissertation few control algorithms are described. Some of these control algorithms are:

(i) Synchronous Reference Frame (SRF) Theory
(ii) Anti-Hebbian (AH) Learning Algorithm
(iii) Character of triangle function (CTF)
(iv) Improved linear sinusoidal tracer (ILST)

4.3 Description of control algorithms

The mathematical description of various control algorithms used in this thesis are described as under

4.3.1 Synchronous Reference Frame (SRF) theory

SRF theory is related to extraction of synchronously rotating d-q components of current from 3-phase load current. A block diagram for this theory is shown in Fig 4.1. Controller is the basic building block of this algorithm. Controller takes source voltage and load current as input. Phase locked loop (PLL) tracks the phase of input voltage signal and

generate unit voltage templates (sine and cosine components). These d-q components of currents passed by a filter which filter out high frequency harmonic components. Then again d-q frame is transformed back to 3-phase components. This current is then compared with source current and error between them is fed to Hysteresis-based PWM signal generator to produce final switching signals which are the pulses for DSTATCOM.

The AC side terminal voltages are given as

$$v_{sa} = V_m \sin(\omega t) \tag{4.1}$$

$$v_{sb} = V_m \sin(\omega t - {}^{2\pi}/_{3}) \tag{4.2}$$

$$v_{sc} = V_m \sin(\omega t + {}^{2\pi}/_{3}) \tag{4.3}$$

and fundamental component of load current are given as:

$$i_{la} = I_m \sin(\omega t - \theta_n) \tag{4.4}$$

$$i_{lb} = I_m \sin(\omega t - {}^{2\pi}/_{3} - \theta_n) \tag{4.5}$$

$$i_{lc} = I_m \sin(\omega t - {}^{2\pi}/_{3} - \theta_n) \tag{4.6}$$

Using equation (4.7), Current components in $(\alpha - \beta)$ coordinates are calculated.

$$\begin{bmatrix} i_\alpha \\ i_\beta \end{bmatrix} = \frac{\sqrt{2}}{3} \begin{bmatrix} 1 & -{}^{1}/_{2} & -{}^{1}/_{2} \\ 0 & {}^{\sqrt{3}}/_{2} & -{}^{\sqrt{3}}/_{2} \end{bmatrix} \begin{bmatrix} i_{la} \\ i_{lb} \\ i_{lc} \end{bmatrix} \tag{4.7}$$

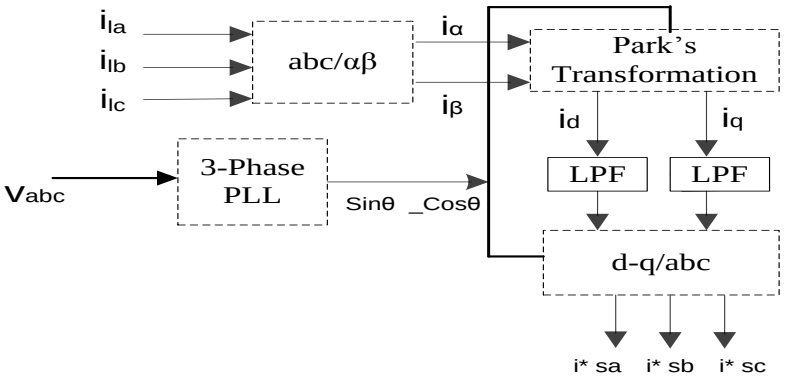

Fig 4.1 Reference current extraction using SRF theory

A PLL is used to determine the transformation angle for converting $(\alpha - \beta)\ to\ (d - q)$ frame. After this, filter is used to remove dc component from the currents, then$(d - q)$ component of current is converted to (α-β), equation (4.8).

$$\begin{bmatrix} i_\alpha^* \\ i_\beta^* \end{bmatrix} = \begin{bmatrix} cos\theta & sin\theta \\ -sin\theta & cos\theta \end{bmatrix} \begin{bmatrix} i_d \\ i_q \end{bmatrix} \tag{4.8}$$

and to convert from($\alpha - \beta$) to a-b-c, equation (4.9) is used.

$$\begin{bmatrix} i_{sa}^* \\ i_{sb}^* \\ i_{sc}^* \end{bmatrix} = \frac{\sqrt{2}}{3} \begin{bmatrix} 1/\sqrt{2} & 1 & 0 \\ 1/\sqrt{2} & -1/2 & \sqrt{3}/2 \\ 1/\sqrt{2} & -1/2 & -\sqrt{3}/2 \end{bmatrix} \begin{bmatrix} i_0 \\ i_\alpha^* \\ i_\beta^* \end{bmatrix} \tag{4.9}$$

These are reference current generated. These reference currents are compared with actual current and error between both will be the required amount of reactive current supplied by DSTATCOM. Error of current is used to generate pulses for inverter. Inverter is equipped with a capacitor, which supplies necessary reactive power to the system.

4.3.2 Anti-Hebbian Learning Algorithm

Neural network is like a human brain with learning capability and generalization. It is used to represent functions as weighted sums of nonlinear terms. It is able to approximate very complicated nonlinear functions, and therefore considered as a universal approximation. Anti-Hebbian control algorithm is basically a neural network technique which is based on TLS for extraction reference currents. For extraction of fundamental Active Power Component of Reference Source Currents unit voltage templates are calculated, as given below.

4.3.2.1 Unit template calculation

Unit amplitude templates are in phase and quadrature component of source voltage, which are of unit magnitude. These templates are used by reference current at the later part of the algorithm. They are used to provide phase difference to different components of current so that they can be compared with actual current for generation of firing pulses. For

calculation of unit amplitude template, first terminal voltage, v_m , is calculated by the formula given in eq.(4.10), where v_a, v_b and v_c are phase voltages of the supply line.

$$v_m = Sqrt(\{(2/3)(v_{sa}^2 + v_{sb}^2 + v_{sc}^2)\}) \quad (4.10)$$

After that individual phase voltages get divided by terminal voltage, this will give unit amplitude with the phase angle of actual supply of phase voltage. In phase components are represented by u_{pa}, u_{pb} and u_{pc} , respectively for phase a, b and c. Quadrature components are represented by u_{qa}, u_{qb} and u_{qc} , respectively for phase a, b and c. Equation for calculation are given below.

$$u_{pa} = \frac{v_a}{v_m},\ u_{pb} = \frac{v_b}{v_m},\ u_{pc} = \frac{v_c}{v_m} \quad (4.11)$$

$$u_{qa} = -\frac{u_{pb}}{\sqrt{3}} + \frac{u_{pc}}{\sqrt{3}} \quad (4.12)$$

$$u_{qb} = \sqrt{3}\frac{u_{pa}}{2} + \frac{(u_{pb} - u_{pc})}{2\sqrt{3}} \quad (4.13)$$

$$u_{qc} = -\sqrt{3}\frac{u_{pa}}{2} + \frac{(u_{pb} - u_{pc})}{2\sqrt{3}} \quad (4.14)$$

Anti-Hebbian learning rule is obtained from the Hebbian rule given by reversing the sign of its incremental term. This is the reason for its name as Anti-Hebbian.

The simplest linear neural model is given by:

$$\eta(t) = \sum_{i=1}^{n+1} \phi_i(t)\, \xi_i(t) \quad (4.15)$$

In this equation $\eta(t)$ is output of neuron, $\xi_i(t)$ is the input vector and $\phi_i(t)$ is the weight vector. In basic hebbian algorithm weight vector is modified by adding to it a small increment that is the proportional to the product of input and output signal. In anti-hebbian as the name described, instead of adding the incremented weight, it is subtracted from the weight vector. The output signal for $\phi_i(t)$ is given as:

$$\widetilde{\phi}_i(t+1) = \widetilde{\phi}_i(t) - \eta(t)\xi_i(t) \quad (4.16)$$

Where, μ is scaling factor. It is a constant term.

By performing the scaling function on the weight vector

$$\widetilde{\phi_i}(t+1)=-1x\frac{\widetilde{\phi_i}(t+1)}{\widetilde{\phi_{n+1}}(t+1)} \tag{4.17}$$

Combining above two equations:

$$\widetilde{\phi_i}(t+1)=\frac{\widetilde{\phi_i}(t)-\mu\eta(t)\xi_i(t)}{1+\mu\eta(t)\xi_{n+1}(t)} \tag{4.18}$$

Numerator of eq.(4.18) shows the anti-hebbian learning operation and the denominator keeps the last component of the weight vector to -1. Anti-Hebbian learning requires weight normalization, in this case to prevent weight vectors from collapsing to zero. Oja's active decay rule (Oja, 1982) is a popular local approximation to explicit weight normalization:

$$\Delta W = \eta(xy - wy^2) \tag{4.19}$$

Here the first term in parentheses (xy) represents the standard Hebb rule, while the second (wy^2) is the active decay. Based on the above equation (4.19) weight of active power component of phase 'a' load current is estimated as

$$W_{pa} = \int \eta\{(i_{da} - u_{spa} W_{pa})(\beta\, i_{la} W_{pa})\}\, dt \tag{4.20}$$

Where, u_{spa} is same as u_{pa} , i.e. in-phase unit template, η is learning rate, β is a constant and

$$i_{da} = (i_{la} - u_{spa} W_{pa}) \tag{4.21}$$

and reactive power component of phase 'a' load current is

$$W_{qa} = \int \eta\{(i_{la} - u_{sqa} W_{qa})(\beta\, i_{la} W_{qa})\}\, dt \tag{4.22}$$

Where u_{sqa} is same as u_{qa}, i.e. in-quadrature unit template. Similarly, for other phases weights are calculated, then average of weights of all the phases will give fundamental active power component of reference current as given in below equation

$$W_{PA}=(W_{pa}+W_{pb}+W_{pc})/3 \tag{4.23}$$

$$W_{QA}=(W_{qa}+W_{qb}+W_{qc})/3 \quad (4.24)$$

Where W_{pb}, W_{pc} are active power component of phase 'b' and 'c' load current and W_{qb}, W_{qc} are quadrature components of phase 'b' and 'c' load currents.

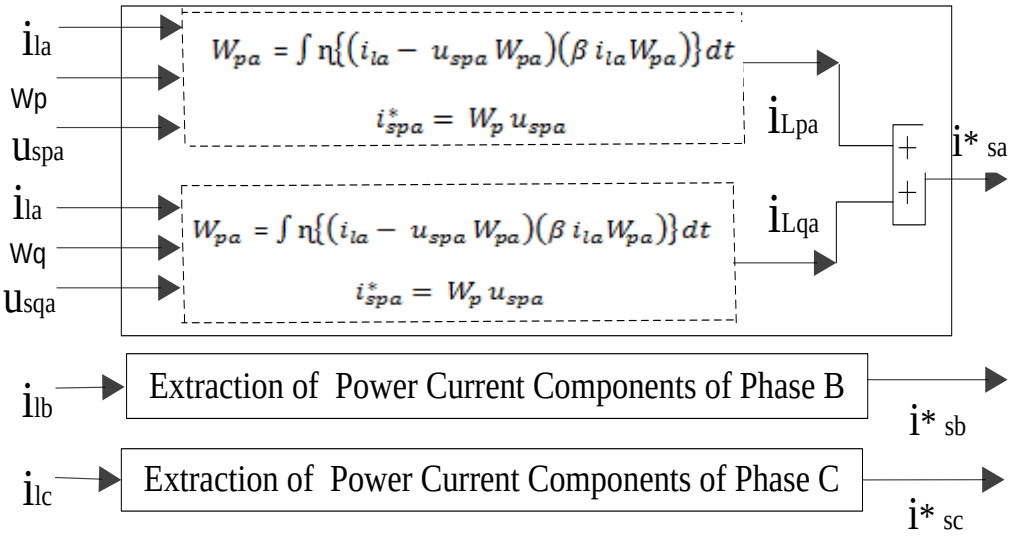

Fig 4.2 Weight estimation using Anti- Hebbian

Total active weight component is calculated by the addition of fundamental active weight component with the output of PI controller used for DC bus voltage maintenance of DSTATCOM and given as $'W_P'$. And total reactive weight component is calculated by the addition of fundamental reactive weight component with the output of PI controller used for PCC voltage maintenance and given as $'W_Q'$.

The three-phase fundamental active power component of reference source currents are calculated as

$$i^*_{sap}= W_P{}^*u_{pa},\ i^*_{sbp}=W_P{}^*u_{pb} \text{ and } i^*_{scp}=W_P{}^*u_{pc} \quad (4.25)$$

4.3.2.2 PI Controllers

There are two PI (Proportional Integral) controllers used in the system. One is for maintaining DC bus voltage. Other is to maintain voltage at PCC within limit. Variation

in DC bus voltage determines the amount of active power needed by inverter for its operation. Error between capacitor voltage and reference voltage is the input to PI controller, output of PI controller added with active component of current.

Other PI controller is for maintaining PCC voltage. So this component is related to the flow of reactive power in the system. Output of PI controller added with reactive component of current.

(i) PI controller for maintaining constant DC bus voltage of DSTATCOM

DSTATCOM system is used to fulfill only reactive power need of the system. On the other hand, a.c. supply has to provide active power as well as the losses occurring in the system because losses are considered to be occur on resistance and which is dissipated in the form of heat. Thus the total active component of load current consists of two parts one is of load demand and other is the losses. To compute second component, a reference DC bus voltage V_{dc}* is compared with actual DC bus voltage, then the error is processed through PI controller. The output at n^{th} sampling instant is given as:

$$I_{dc(n)}=I_{dc(n-1)}+k_{P1}\{v_{dce(n)} - v_{dce(n-1)}\}+k_{I1}v_{dce(n)} \quad (4.26)$$

Where, k_{P1} is proportional gain and k_{I1} is derivative gain. This current is account for the total loss of DSTATCOM.

(ii) PI controller for maintaining PCC voltage:

For maintaining PCC voltage constant, a PI controller is used which takes the error between actual voltage and reference voltage as input and produces a reactive component of current, which get added with reactive component of load current. So this reactive power needed to maintain PCC voltage is supplied by DSTATCOM.

$$i_{coq(n)}= i_{coq(n-1)}+ k_{P2}\{v_{m(n)} - v_{m(n-1)}\}+ k_{I2}v_{m(n)} \quad (4.27)$$

Where, $i_{coq(n)}$ is output of PI controller, v_m is terminal peak voltage, k_{P2} and k_{I2} are proportional and integral controller gain.

4.3.2.3 Switching Signal generation

Switching signal for inverter is obtained by two methods, one is pulse width modulation (PWM), in this method actual current is compared with a triangular reference waveform to generate pulses. Frequency of carrier wave depends on sampling time of system.

Other method is Hysteresis current controller (HCC) in which a band is defined, if value of current exceeds upper limit of that current than pulses will be present and when amplitude of current goes lower than limit output will be zero.

4.3.3 Character of triangle function (CTF) approach

For pure sinusoidal voltage, only the fundamental component of the current contributes in real power transfer. Load current $i_L(t)$ is comprised of fundamental load current (I_{L1}) and harmonic currents (i_H).

$$i_L(t) = i_{L1} + i_H + i_{dc} \tag{4.28}$$

i.e.

$$i_L(\text{t})=\sqrt{2}I_{L1}\sin(\omega t + \emptyset_{i1})+\sum_{n=1}^{\infty}\sqrt{2}I_L \sin(n\omega t + \emptyset_{in}) + i_{dc} \tag{4.29}$$

In above eq. , I_{L1} and $\emptyset_{i1}$ are RMS values of fundamental component of current and phase angle respectively. By expanding above eq., we get

$$i_L(\text{t})= \sqrt{2}I_{L1}\sin(\omega t)\cos(\emptyset_{i1})+\sqrt{2}I_{L1}\cos(\omega t)\sin(\emptyset_{i1}) + \sum_{n=1}^{\infty}\sqrt{2I_L} \sin(n\omega t + \emptyset_{in})+I_{dc}$$

(4.30)

Fundamental load component can be expressed as the sum of active and reactive component of current.

$$i_{L1} = i_{Lp} + i_{Lq} \tag{4.31}$$

Eq. (4.28), becomes

$$i_L(t) = \ i_{Lp} + \ i_{Lq} + \ i_H + \ i_{dc} \tag{4.32}$$

Where i_{Lp}, i_{Lq}, i_H and I_{dc} are load fundamental active current, reactive current, harmonic current and DC current components respectively.

Maximum values of load fundamental current component are along horizontal and vertical axis. This leads to represent fundamental current component as

$$I_{Lp} = \sqrt{2} I_{L1} \cos(\emptyset_1) \tag{4.33}$$

$$I_{Lq} = \sqrt{2} I_{L1} \sin(\emptyset_1) \tag{4.34}$$

From eq. (4.33),(4.34) and (4.32), we get

$$i_L(t) = \ I_{Lp} \sin(\omega t) + I_{Lq} \cos(\omega t) + i_H + \ i_{dc} \tag{4.35}$$

Multiply both sides with {2sin(ωt)}, we get

$$2 \sin(\omega t)\, i_L(t) = \ I_{Lp}(1 - \cos(2\omega t)) + I_{Lq} \sin(2\omega t) + i_H(2\sin(\omega t)) \tag{4.36}$$

This equation is based on character of triangle function. From this eq., fundamental component of active current can be found out with the help of low pass filter. To design this control algorithm, following steps are followed:

4.3.3.1 Estimation of load fundamental component of active and reactive current

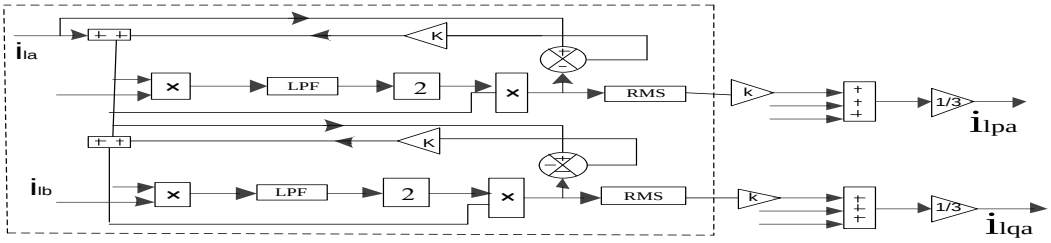

Fig 4.3 Extraction of load current using CTF

Load fundamental active component of current is subtracted from original current, this will estimate reactive and harmonic current. A constant value which is the % of harmonic and active current are added with polluted current. Then this factor is multiplied with in- phase component to voltage. After suppressing the harmonics and other component by LPF, this component is again multiplied by a factor of 2. This will give fundamental active component of load current. This value of current is RMS, to convert this value to peak component 1.414 is multiplied to this. Similar calculation is done for phase b and c.

Load fundamental reactive component of current is subtracted from original load current, this will estimate active and harmonic current. A constant value which is the % of harmonic and reactive current are added with polluted current. Then this factor is multiplied with quadrature component to voltage. After suppressing the harmonics and other component by LPF, this component is again multiplied by a factor of 2. This will give fundamental reactive component of load current. This value of current is RMS, to convert this value to peak component 1.414 is multiplied to this. Similar calculation is done for phase b and c.

Then average active current component can be calculated as given in below equation:

$$I_{LA}=(I_{pa}+I_{pb}+I_{pc})/3 \quad (4.37)$$

$$I_{QA}=(I_{qa}+I_{qb}+I_{qc})/3 \quad (4.38)$$

Total active current component is calculated by the addition of fundamental active current component with the output of PI controller used for DC bus voltage maintenance of DSTATCOM.

4.3.4 Adaptive filter based Improved Linear Sinusoidal Tracer (ILST)

An adaptive sinusoid tracer uses least square error, gradient descent method and rotation transform to estimate the instantaneous value and amplitude of sinusoid. It has the advantage of selectable frequency and bandwidth parameters. Block diagram of LST is shown in fig.4.4.

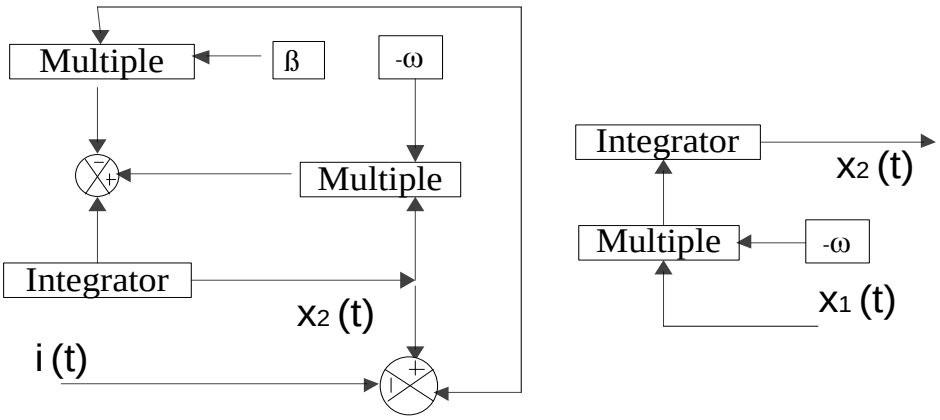

Fig 4.4 Block diagram of LST

In this method, fundamental component of load current, both in-phase and 90-degree shifted is estimated. Fig 4.4 shows $i(t)$ as load current, $x_1(t)$ and $x_2(t)$ as estimation of fundamental current in-phase and shifted 90-degree waveform respectively. Here, α and β are parameters of filter and frequency. Transfer function of above system can be written as:

$$C(s) = \frac{s^2 + \alpha^2}{s^2 + \beta s + \alpha^2} \tag{4.39}$$

when α = ω_0, i.e. the frequency of fundamental current, this system is a second-order notch filter. β should be adjusted according to input frequency, to adjust bandwidth of the system, such that harmonic components get filter out. Prime disadvantage of the system is that if difference between actual current component and estimated component contains high order harmonics then stability of the system decreases. To overcome this difficulty, a low-pass filter is added to the system, this improves the system stability. Transfer function of low-pass filter is:

$$C_{LPF}(s) = \frac{1}{\tau s + 1} \tag{4.40}$$

Where τ is time constant of filter, which decides amount of time delay provided by filter.

From fig.4.5, overall transfer function of the system becomes,

$$C_{total}(s) = \frac{(\tau\alpha^2 + \beta)s}{\tau s^3 + s^2 + (\tau\alpha^2 + \beta)s + \alpha^2} \tag{4.41}$$

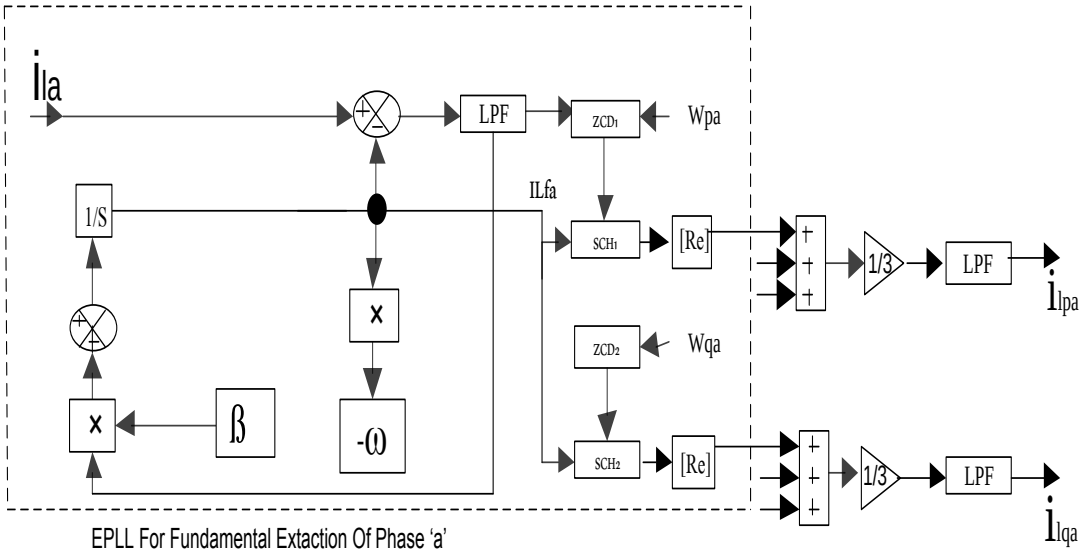

Fig 4.5 Fundamental current extraction using ILST

This system represents a stable system, whose stability can be checked by Routh-Hurwitz criteria.

For extraction of three-phase fundamental load active power component of current, zero crossing detector (ZCD) is used as a trigger pulse of sample and hold (SHC) circuit. SHC_1 output is fundamental active component of load current. Then average active current component can be calculated as given in below equation

$$i_{LA}=(i_{pa}+i_{pb}+i_{pc})/3 \tag{4.42}$$

Similarly, for calculation of reactive power component of fundamental load current zero crossing of quadrature unit template phase is used. ZCD is used as trigger circuit for SHC_2. Output of SHC2 is fundamental reactive power component of load current. Then average active current component can be calculated as given in below equation

$$i_{QA}=(i_{qa}+i_{qb}+i_{qc})/3 \tag{4.43}$$

Similar calculation is for other phases to determine both active and reactive component of current.

4.4 Conclusion

In this chapter, a detailed description of various control algorithms is presented. By analyzing approach of control algorithms, we conclude that SRF is based on axis transformation, which is basic approach. In this approach PLL is used, which introduces some time delay in system. This time delay can create a problem in real time implementation of SRF theory. This time delay is reason for heavy amount of current flow in the system. In real time SRF theory is used only when time delay is less. Anti-Hebbian is a neural network based technique. This technique extracts fundamental component of reference current. Neural network technique increases accuracy of system. Anti- Hebbian is good technique in terms of performance. CTF is a basic technique which introduces very less time because of components used in this approach. ILST is improved version of basic linear sinusoidal tracer. This modification helps to increase reliability of system.

CHAPTER 5

SIMULATION AND EXPERIMENTAL RESULTS

This chapter presents simulation analysis and hardware realization of a DSTATCOM unit for harmonic and reactive power compensation in a non-linear load using some intelligent control algorithms. In this chapter Synchronous reference frame (SRF) theory, Anti-Hebbain learning algorithm, character of triangle function (CTF) and improved linear sinusoidal tracer (ILST) based control algorithms are implemented for elimination of harmonics in source current and comparison on the basis of total harmonic distortion in source current with all four control algorithms are summarized.

5.1 System Configuration

Fig 5.1 shows schematic diagram of distribution system feeding a non-linear load and supported with DSTATCOM.

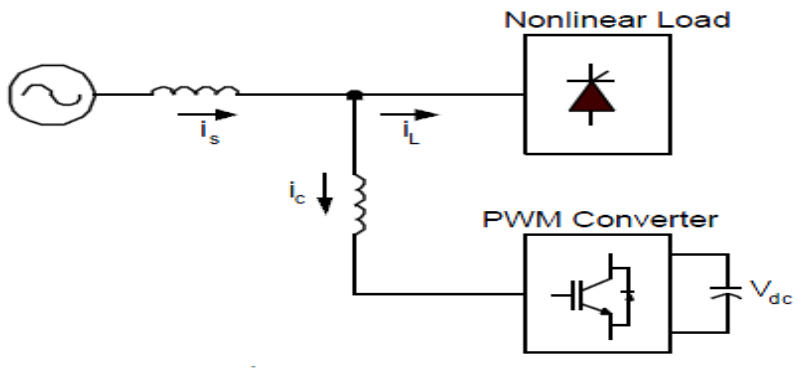

Fig 5.1 Schematic diagram of distribution system

The three-phase supply system is an ideal sinusoidal voltage source; but due to diode bridge rectifier the load current is non sinusoidal and distorted and contains harmonic components. The DSTATCOM is a three phase voltage source converter (VSC) with a seif supported DC bus capacitor. If battery is connected at dc side of DSTATCOM, it will supply active power only but to supply reactive power capacitor should be used. In this dissertation work only reactive power is supplied by DSTATCOM.

5.2 MATLAB Simulation model of DSTATCOM

MATLAB Simulation model is designed for the distribution system. Fig 5.2 shows MATLAB Simulation model for distribution system. In this system, three phase ideal source is supplying power to non-linear load. Non-linear load is shown by three-phase diode rectifier module connected to resistor-inductor (R-L) load. The DSTATCOM is an IGBT based three-phase voltage source converter. This converter is controlled to supply needed reactive power and harmonic current into the system. To interface DSTATCOM to distribution system, filter inductors are used. These inductors are used to limit circulating current flowing in the system.

To control the amount of power flow from DSTATCOM, SRF theory, Anti-Hebbain, CTF and ILST based control algorithms (shown by controller in the system) are designed.

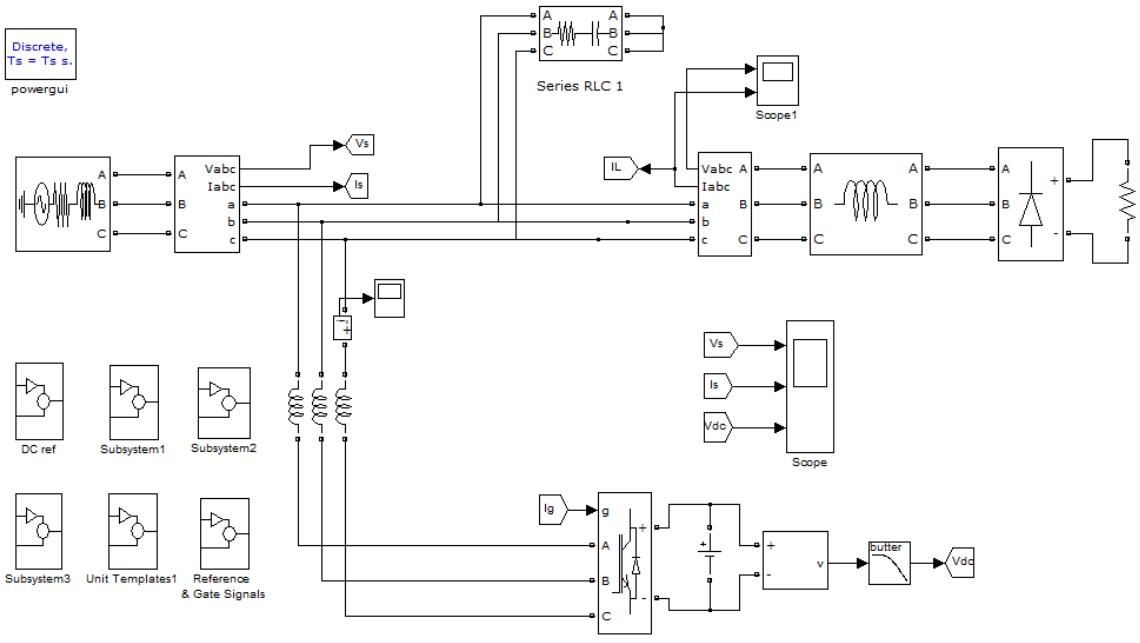

Fig 5.2 MATLAB model of distribution system

These control algorithms are based on different approaches. A MATLAB model of the system is developed in simulink. The value of system parameters are described in

Appendix A. Simulation is carried out in discrete mode at a maximum step size of 1x 10^{-6} with ode45 (Dormand-Prince).

A combination of resistor and capacitor is used to filter higher order harmonics of the system. The voltage across a capacitor, connected at DC side of VSC is measured and compared with a desired level and regulated to the reference value through a proportional and integral (PI) controller under different operating conditions. Time taken to maintain dc bus voltage of DSTATCOM is tracking time of the system. Less tracking time shows high efficiency of the system.

5.3 Control algorithm design

The simulation and hardware implementation of four control algorithms SRF, Anti-Hebbian, CTF and ILST based control algorithms are demonstrated through MATLAB simulation and hardware implementation using dSPACE respectively.

5.3.1 MATLAB Simulation of Synchronous Reference Frame (SRF) Theory based control algorithm

Three phase source voltage (v_{abc}) is processed by PLL. Output of PLL is unit voltage template ($\sin\theta$ and $\cos\theta$). Load current (i_L) signals are transformed to d-q frame using Park's transformation.

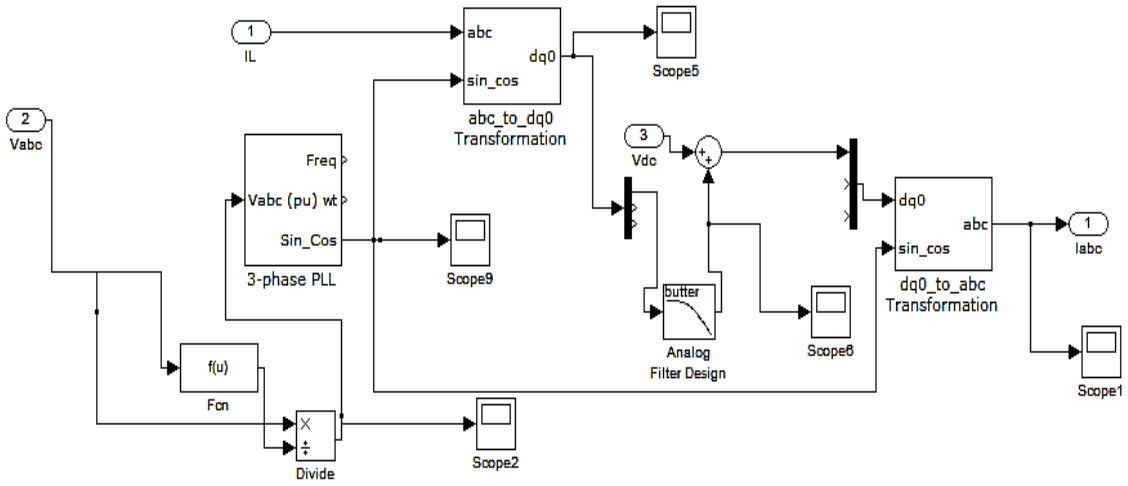

Fig 5.3 SRF Controller for reference current extraction

A low pass filter (LPF) with cut-off frequency 100Hz is used to filter active and reactive current component. The real power required to maintain the voltage of d.c. link capacitor is supplied from VSC by adding the output of the PI controller on d.c. side to the direct current component (i_d) . The resultant i_d and i_q are further transformed to three-phase a-b-c component as a reference current for generating switching signals.

Filtered current signals are converted to a-b-c frame ($i_{sa}^*, i_{sb}^* \text{and} i_{sc}^*$) using Reverse park's and Clark's transformation, which is fed to hysteresis controller for generating switching signal for the VSC.

5.3.1.1 Results and Discussions

Synchronous Reference Frame (SRF) Theory based control algorithm is designed to eliminate harmonics of source current. To calculate the amount of compensation provided by DSTATCOM, total harmonic distortion (THD) of source current is determined using FFT window of MATLAB before compensation and after compensation.

(i) Simulation Results

A three-phase distribution system operating at voltage level of 415V (L-L) is considered for simulation study of the all four control algorithms. Load of 16 kVA is supplied by the supply system. Before connecting DSTATCOM, THD in source current is 24.3% as shown in Fig 5.4. After providing compensation by DSTATCOM, THD is 3.38% as shown in Fig 5.5. According to IEEE standard THD limit for distribution system is 5%. This reduction shows that SRF is good in terms of harmonic reduction.

For analyzing tracking capability of algorithm, load of 16kVA is suddenly increased to 32kVA at 0.3sec as shown in Fig 5.6. Due to switching of additional load on distribution network, the dc side voltage is momentarily dips but PI controllers help to maintain this voltage again.

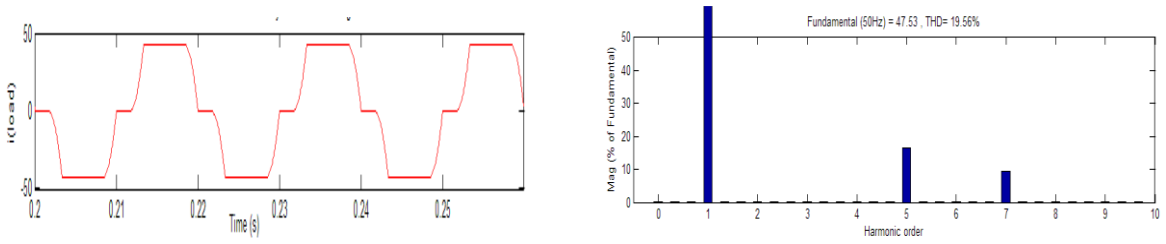

Fig 5.4 THD of source current before compensation

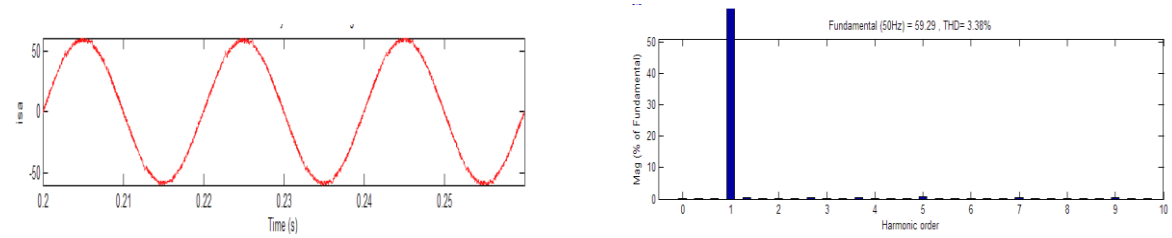

Fig 5.5 THD of source current after compensation using SRF theory based controller

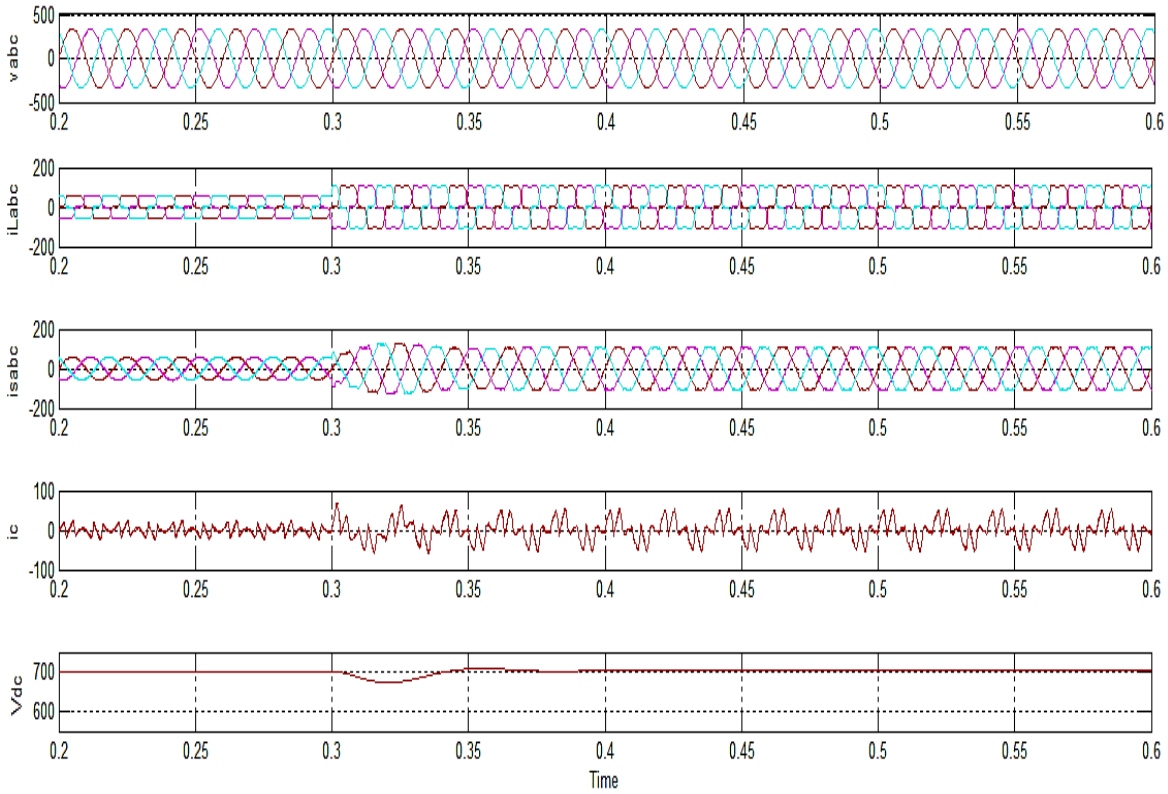

Fig 5.6 Performance of DSTATCOM with SRF Controller while sudden switching of additional load at t=0.3sec and waveform of 3-phase line voltage (v_{abc}), 3-phase load current (i_{Labc}), 3-phase source current (i_{sabc}), Compensating current (i_c) and DC link voltage (V_{dc}).

(ii) Experimental Results

Real time implementation of distribution system is done. Operating voltage of the system is 115V (rms). DC bus voltage is maintained at 200V. Fig 5.7 shows THD of source current before providing compensation by DSTATCOM.

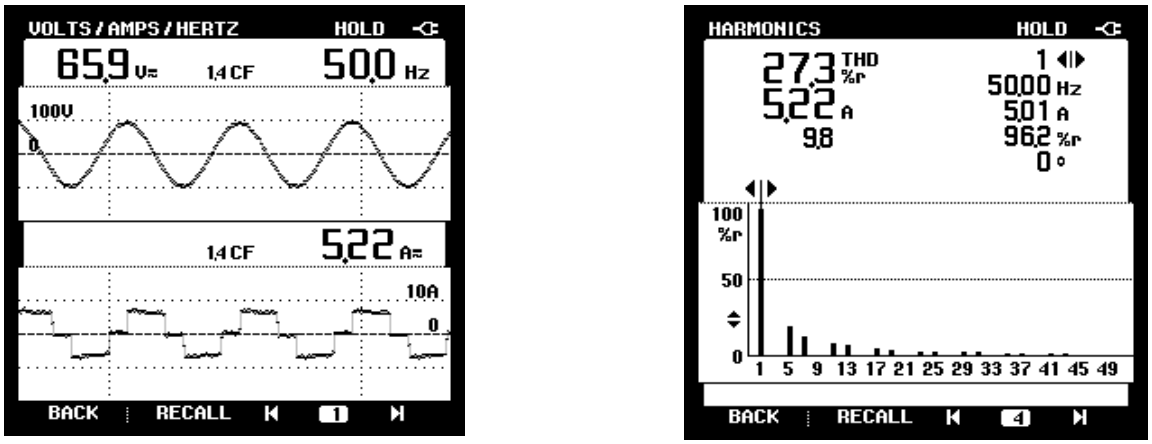

Fig 5.7 Source current and THD of source current before compensation

The VSC in DSTATCOM acts as controlled current source. dSPACE is being used to convert the Simulink model of the control algorithms into real time switching signals for VSC. Fig 5.7 shows current of 5.22A is flowing in the system and waveform of source current is not sinusoidal. This current contains various harmonic components. Also the orders of harmonics present in source current are odd.

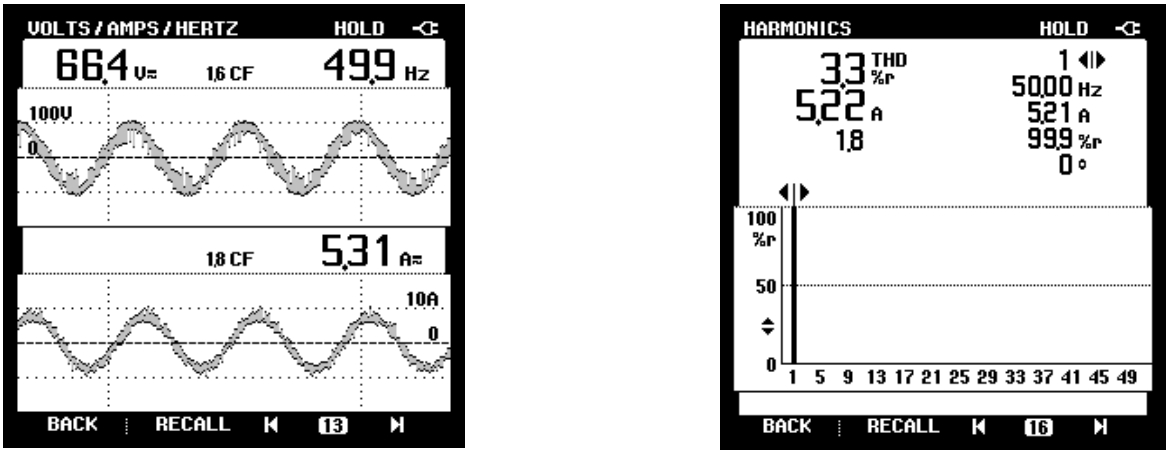

Fig 5.8 Source current and its THD after compensation using SRF theory

Source current after compensation is shown in Fig 5.8. THD of source current reduces to 3.3%. Frequency spectrum of source current shows, magnitude of frequency component other than fundamental is negligible.

Along with current, there is a considerable amount of harmonic present in system voltage.

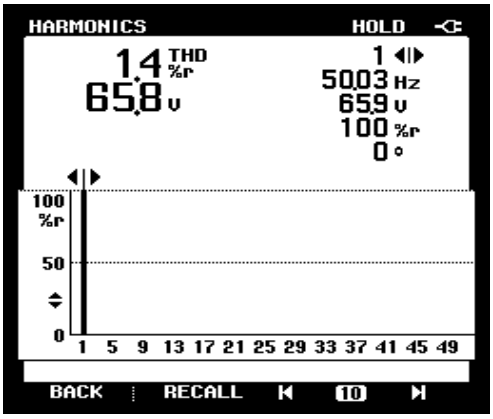

Fig 5.9 THD in voltage using SRF theory

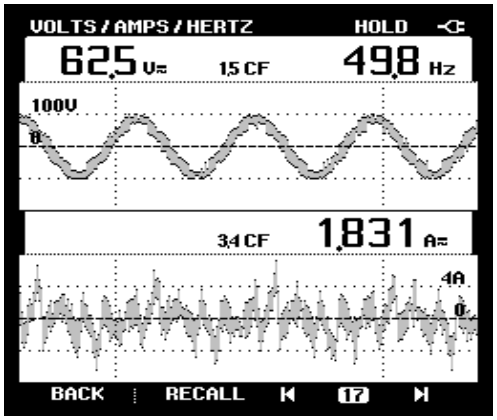

Fig 5.10 Compensating current using SRF theory

Fig.5.9 shows THD of system voltage. It is coming 1.4% which is negligible.

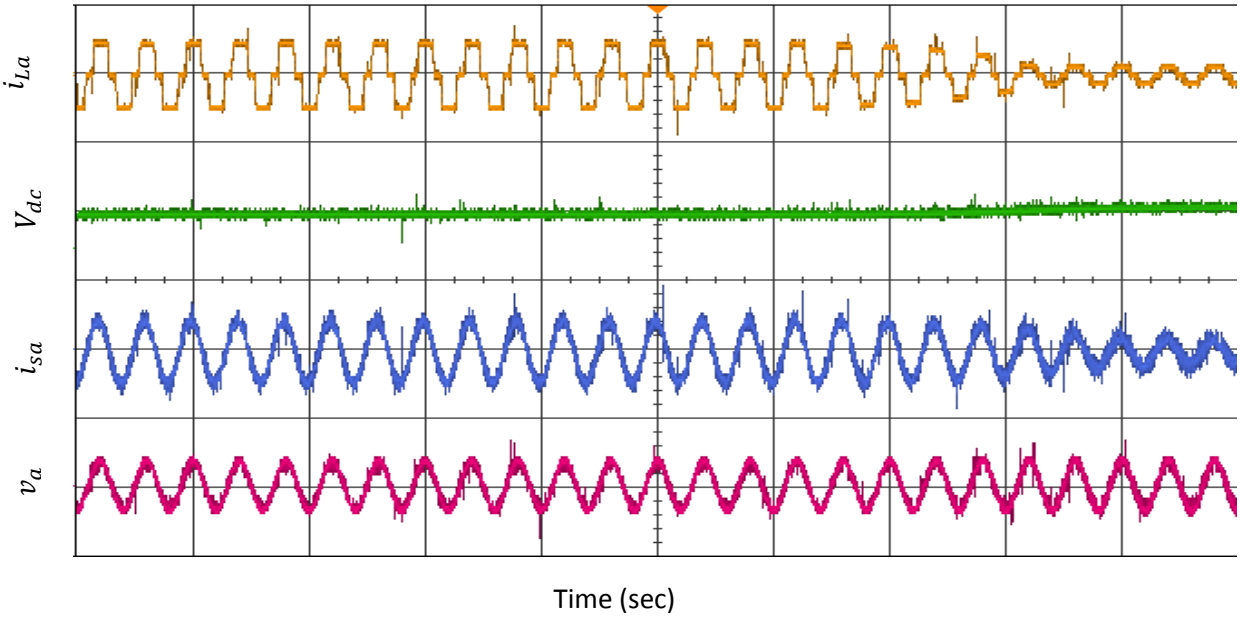

Fig 5.11 Experimental performance of DSTATCOM with SRF control and waveform of Load current (i_{La}), DC bus voltage (V_{dc}), Source current (i_{sa}) after compensation and PCC voltage (v_a)

A current flow from DSTATCOM to system is known as compensating current. Fig 5.10 shows magnitude and waveform of compensating current.

Fig 5.11 shows behavior of system when load is suddenly changed in the system. The load current, dc bus voltage, source current after compensation and voltage at PCC are shown. This figure shows that source current changes from non sinusoidal nature to sinusoidal by providing compensation.

5.3.2 MATLAB Simulation of Anti-Hebbian Learning based control Algorithm

In this algorithm, first step is calculation of in phase and quadrature unit templates of voltage from three-phase source voltage (v_{abc}). Terminal voltage at PCC is calculated by eq. (4.1).

The block in fig 5.12 is designed by using eq. 4.2 to 4.8. When phase voltage is divided by terminal voltage in phase component with unit magnitude is determined. Similarly for other phases unit magnitude template is obtained. Quadrature component is calculated by using in phase component as shown in Fig 5.12.

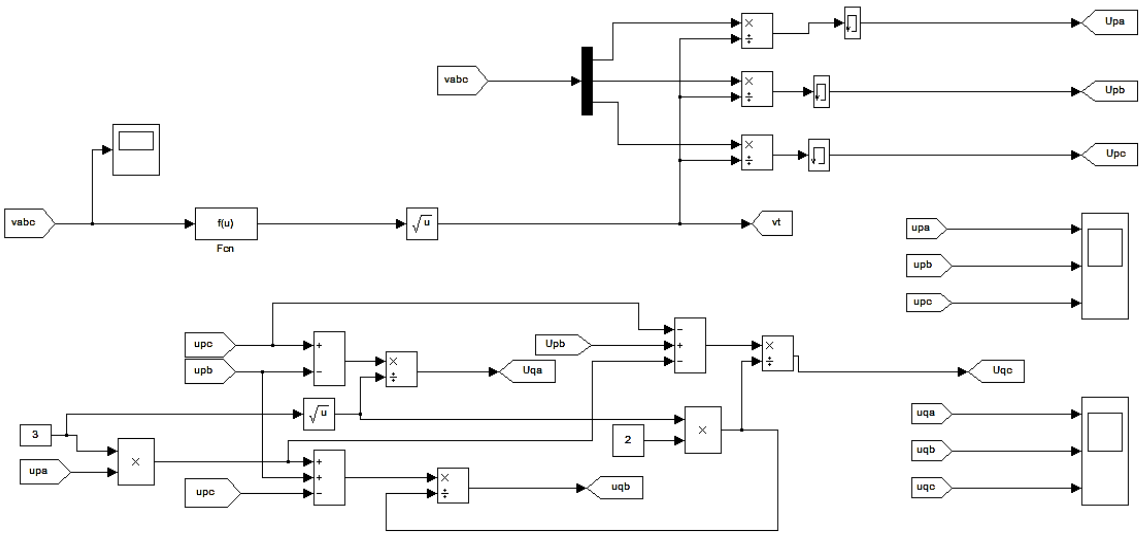

Fig 5.12 In phase and quadrature unit template calculation block

In Anti-Hebbian based learning algorithm, main function is the extraction of weight of fundamental active power component of load current. Fig 5.13 shows reference current estimation of a phase using Anti-Hebbian algorithm based on total least square.

This figure is based on eq. 4.22. In this figure weight of fundamental active power component (W_p) is calculated by load current (i_L). Weight of individual phase component is multiplied by unit template (u_p) of that phase to produce active and reactive load current component.

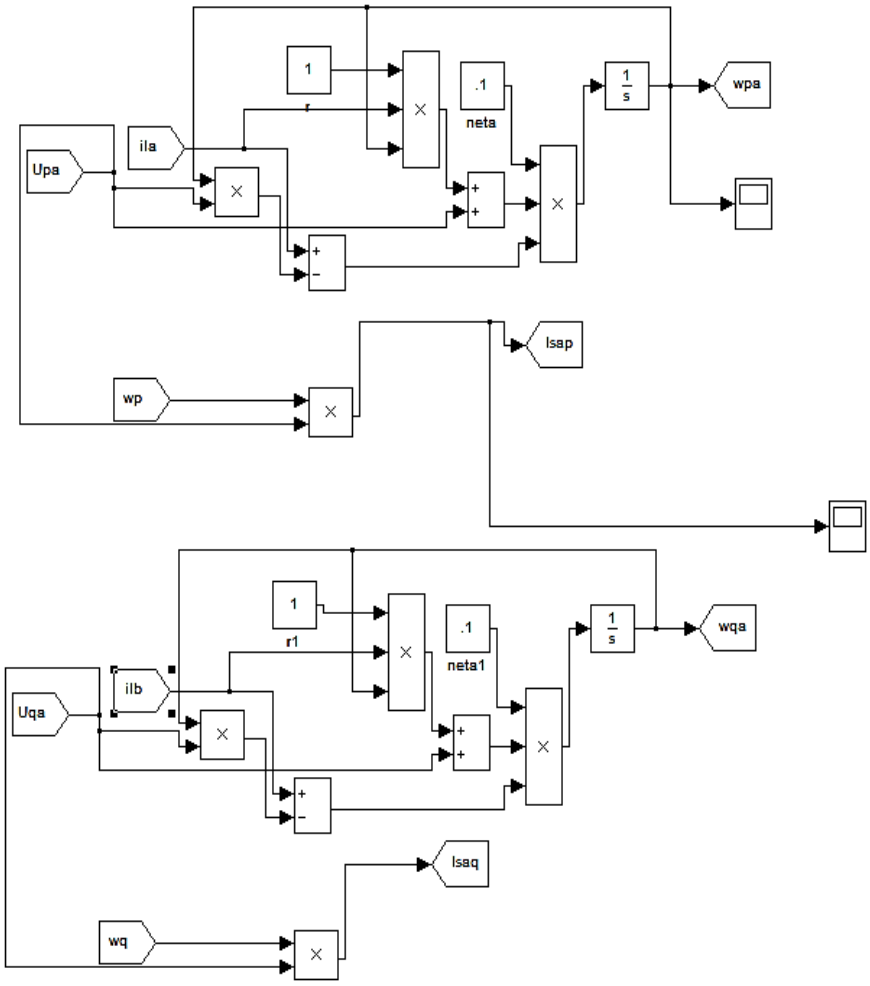

Fig 5.13 Reference current generation of using Anti-Hebbian for phase 'a'

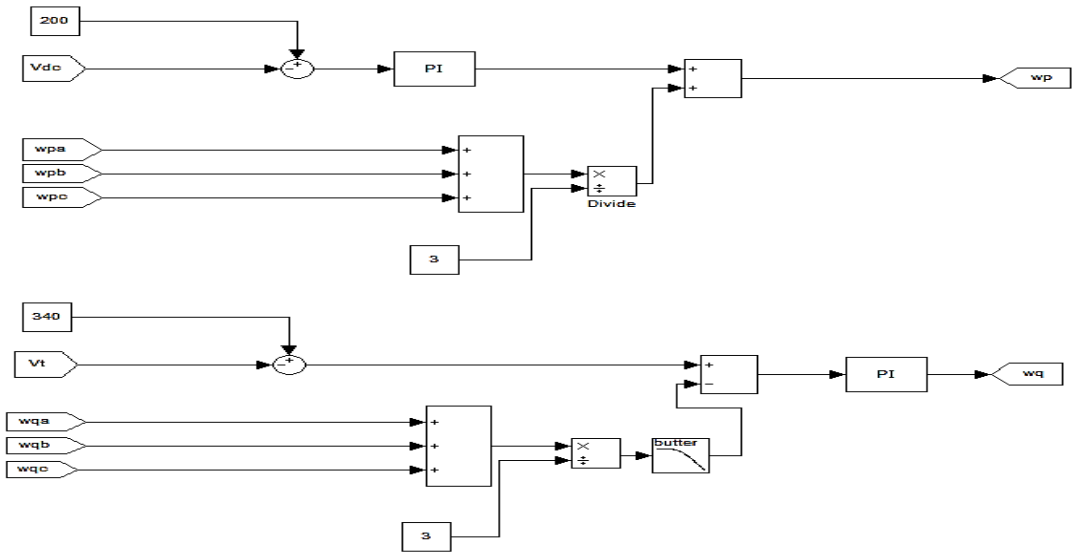

Fig 5.14 PI Controller (a) maintaining DC bus voltage (b) for PCC voltage regulation

Active power demanded by DSTATCOM is also supplied by three-phase source. Difference between reference dc voltage and actual dc voltage is applied to PI controller as shown in Fig 5.14. Output of PI controller is amount of active power component of current drawn by VSC. This component of current is added to the amount of active power current component of circuit, to generate total active current component.

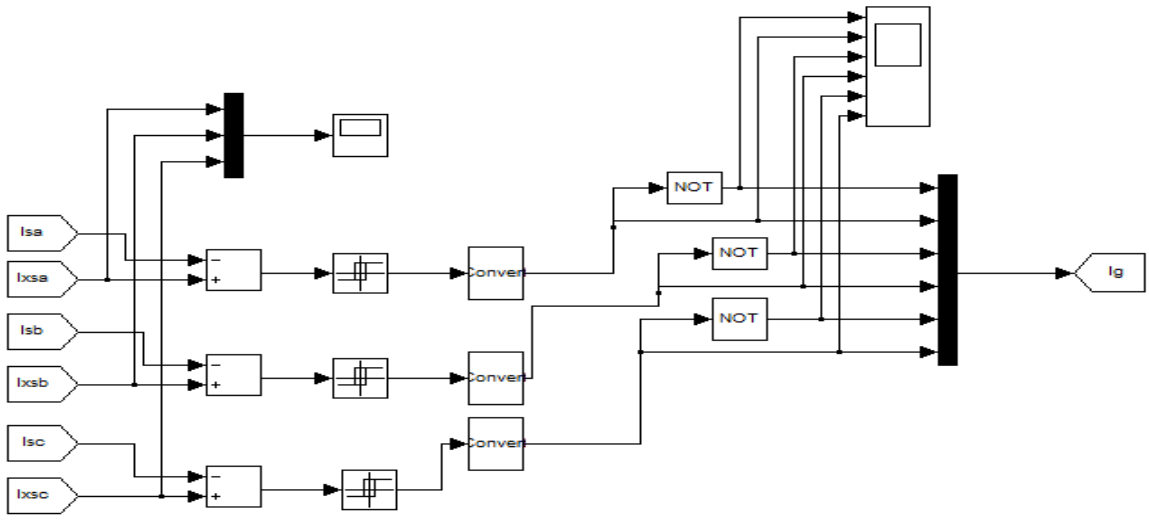

Fig 5.15 Reference current generation and switching signal generation for VSC

For reference current generation, active and reactive fundamental current component is subtracted from source current, as shown in Fig 5.15. This difference of current is supplied by DSTATCOM. Hysteresis current controller is used to generate firing pulse for DSTATCOM.

5.3.2.1 Results and Discussions

Anti-Hebbian based control algorithm is designed to eliminate harmonics of source current. To calculate the amount of compensation provided by DSTATCOM, total harmonic distortion (THD) of source current is calculated using FFT window of MATLAB before compensation and after compensation.

(i) Simulation Results

The distribution system is designed for operation at a voltage level of 415V (L-L). Load of 16 kVA is supplied by the system. Before connecting DSTATCOM, THD of source current is coming 24.3% as shown in Fig 5.4.

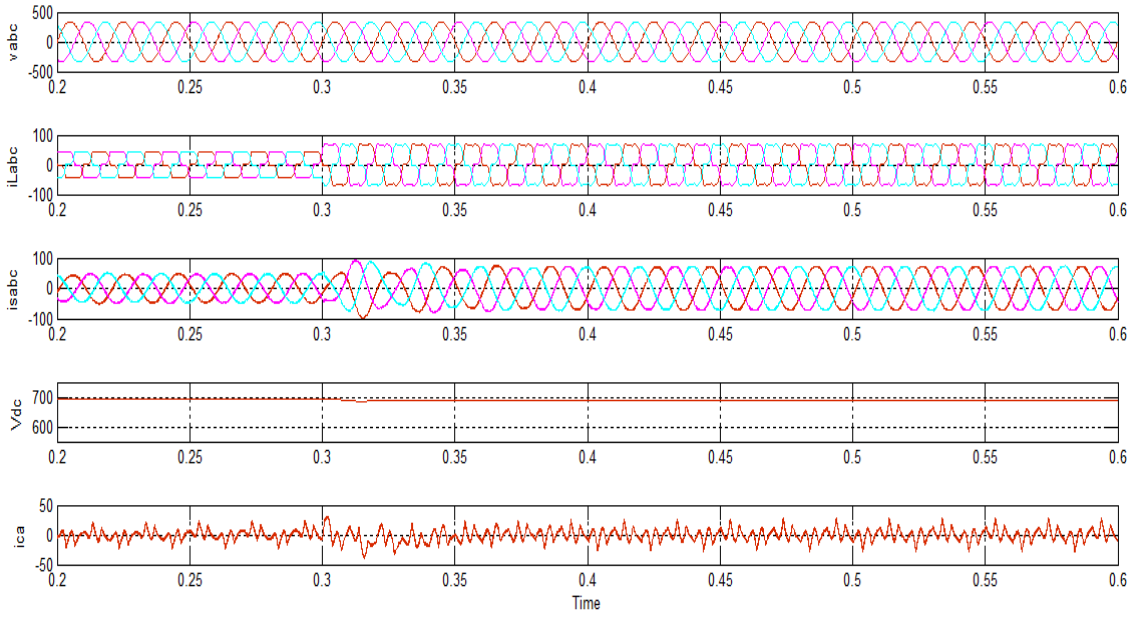

Fig 5.16 Performance of DSTATCOM with Anti-Hebbian Controller while sudden switching of additional load at t=0.3sec and waveform of 3-phase line voltage (v_{abc}), 3-phase load current (i_{Labc}), 3-phase source current (i_{sabc}), DC link voltage (V_{dc}) and Compensating current (i_{ca}).

For analyzing tracking capability of d.c. bus voltage PI controller load of 16kVA is increased to 32kVA. As shown in Fig 5.16, at 0.3 sec load is increased suddenly. Approximately 0.1 sec of time is taken by controller to maintain its voltage again constant after disturbance.

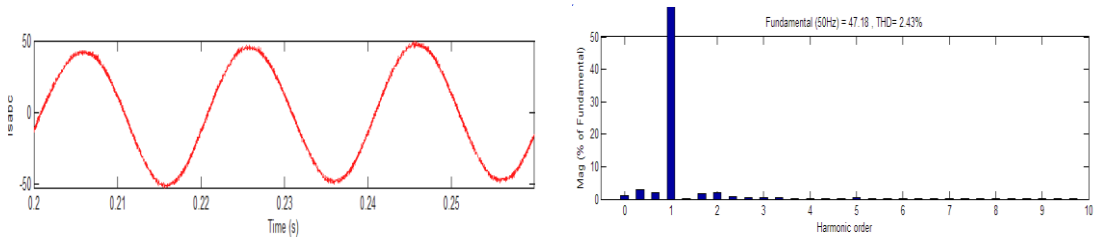

Fig 5.17 Source current waveform and THD with DSTATCOM operation using Anti-Hebbian based control algorithm

After providing compensation by DSTATCOM, THD is coming 2.43% which is less than SRF based controller as shown in Fig 5.17.

(ii) Experimental Results

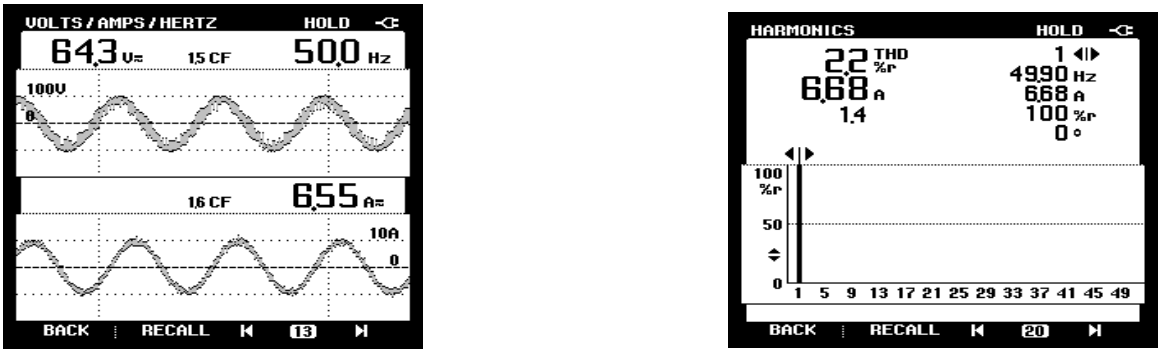

Fig 5.18 Source current and its THD after compensation using Anti-Hebbian algorithm based controller

Fig 5.18 shows compensation of source current using Anti-Hebbian learning algorithm in real time operation of DSTATCOM. THD of source current reduces to 2.2%.

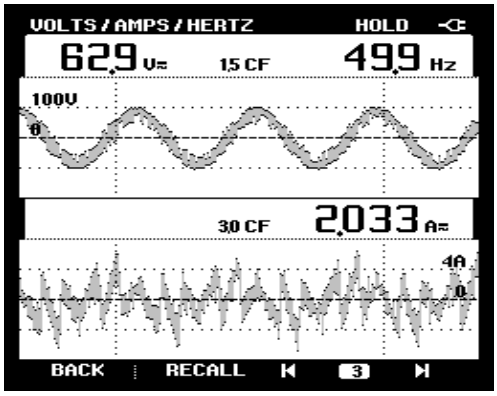

Fig 5.19 Compensating current using Anti-Hebbian learning algorithm based controller

Compensating current injected in to the system during compensation is shown by Fig 5.19. In Fig 5.20, A four channel CRO results are shown. In this figure shown, load is changed suddenly and its effect on load current, dc bus voltage, source current and source voltage is shown.

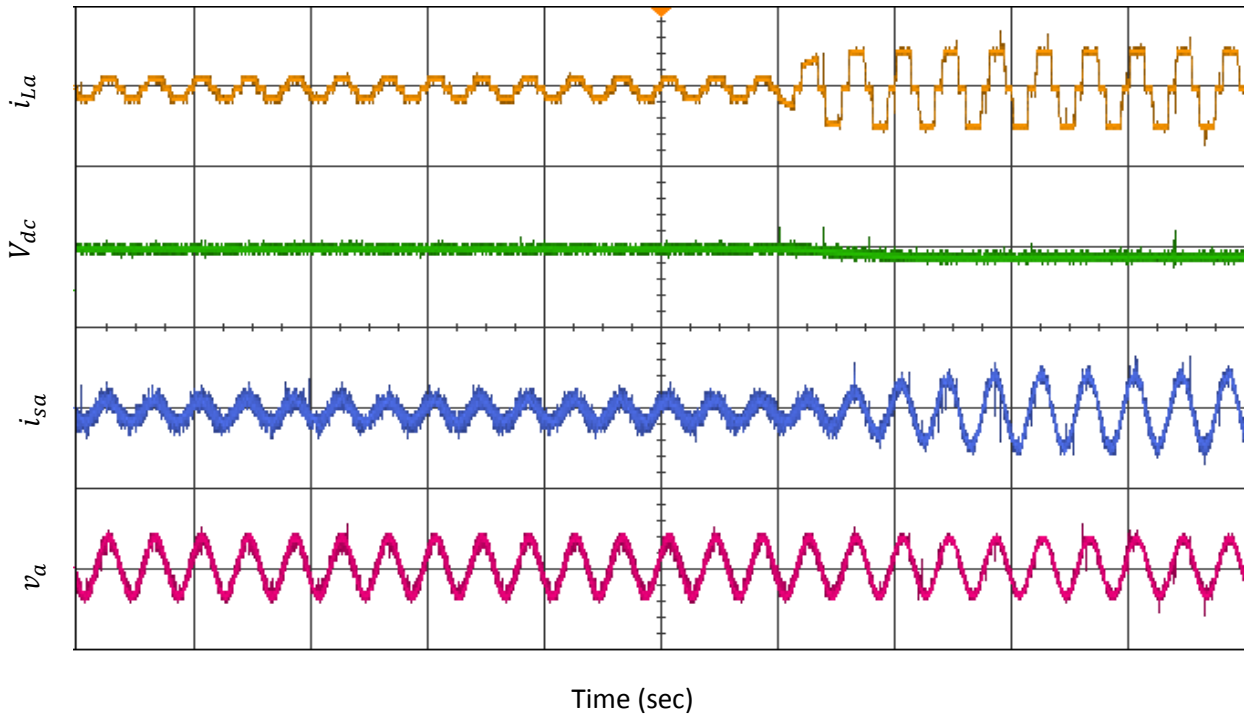

Fig 5.20 Experimental performance of DSTATCOM with Anti-Hebbian control and waveform of Load current (i_{La}), DC bus voltage (V_{dc}), Source current (i_{sa}) after compensation and PCC voltage (v_a)

5.3.3 MATLAB Simulation of Character of Triangle Function (CTF) based control algorithm

CTF based control algorithm is designed by using basic mathematics. By using simple equation (4.36), reference current estimator block can be designed.

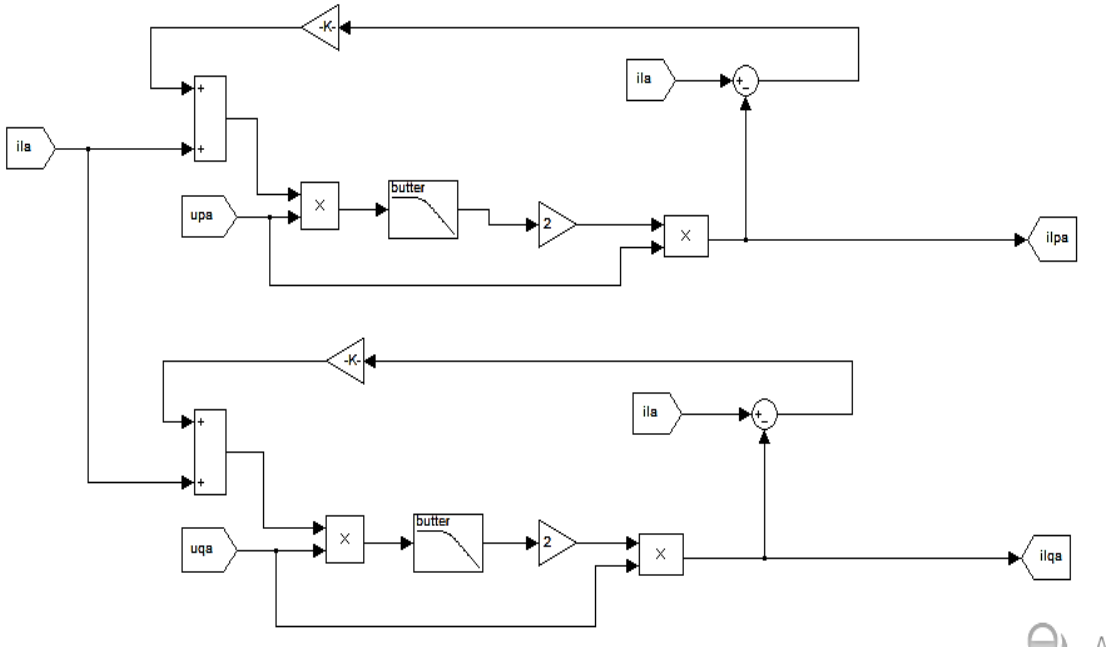

Fig 5.21 Active and reactive current component of one phase using CTF

For filtering higher order terms of eq. 4.36, low pass filter of cut-off frequency 50Hz is used The actual load current of phase 'a' (i_{La}), fundamental active and reactive current component are extracted using filters, summers and multipliers as shown in Fig 5.21.

5.3.3.1 Results and Discussions

CTF based control algorithm is designed to eliminate harmonics of source current. To calculate the amount of compensation provided by DSTATCOM, total harmonic distortion (THD) of source current is calculated using FFT window of MATLAB before compensation and after compensation.

(i) Simulation Results

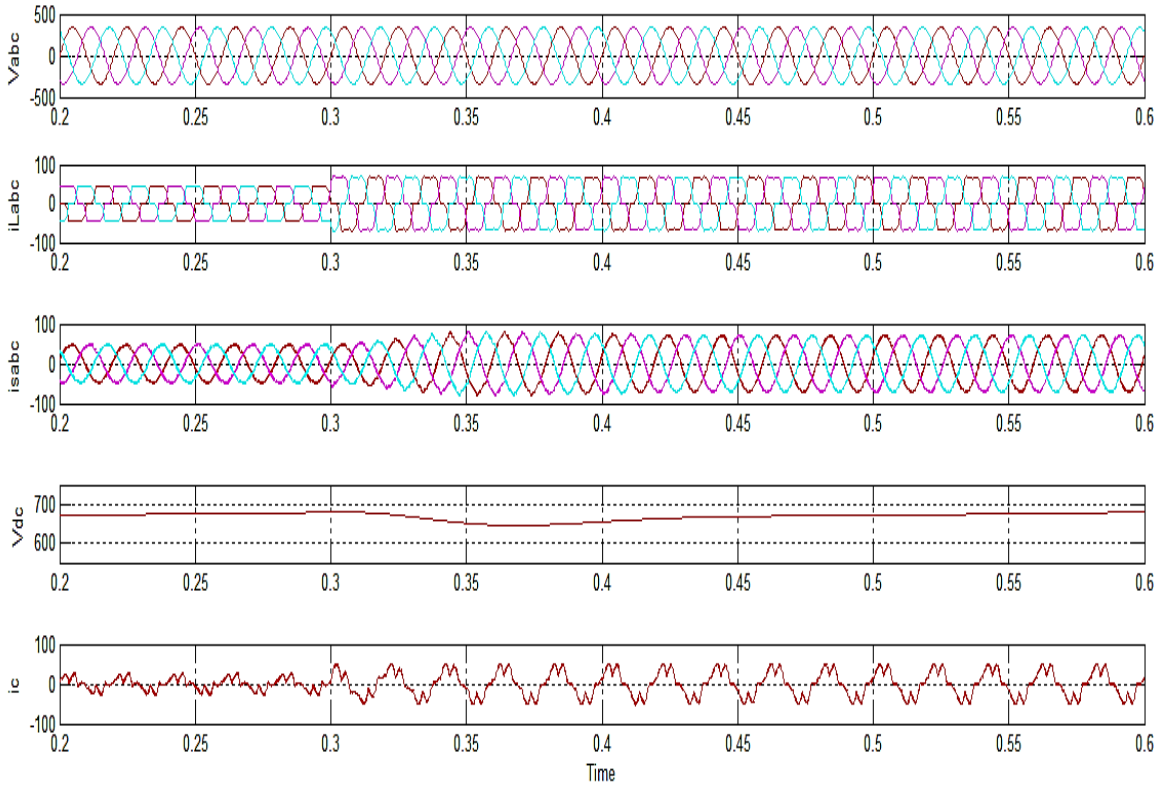

Fig 5.22 Performance of DSTATCOM with CTF controller while sudden switching of additional load at t=0.3sec and waveform of 3-phase line voltage (v_{abc}), 3-phase load current (i_{Labc}), 3-phase source current (i_{sabc}), DC link voltage (V_{dc}) and Compensating current (i_{ca}).

CTF controller is used for harmonic current compensation. In Fig 5.22, dynamic performance of DSTATCOM using CTF based current extractor is shown.

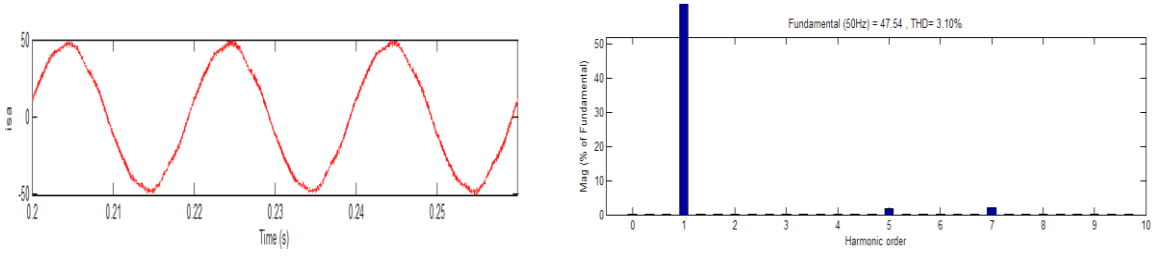

Fig 5.23 Total Harmonic Distortion for source current after compensation

At t=0.3sec load is increased suddenly (i.e. 32kVA from 16kVA). About 0.3 sec is required to recover the dip of DC Bus voltage. Fig 5.23 shows THD of source current after compensation provided by CTF based controller used in DSTATCOM.Due to the presence of non-linear load, source current get distorted. In Fig 5.4 THD for source current is shown as 23.60%. By using CTF technique this THD has been reduced to 4.2%, at the level of 4.5A current.

(ii) Experimental Results

Figure 5.24 shows system behavior, when load is suddenly changed in the system. In this figure, load current, dc bus voltage, source current after compensation and voltage at PCC is shown. This figure shows that source current changes from non sinusoidal nature to sinusoidal by providing compensation.

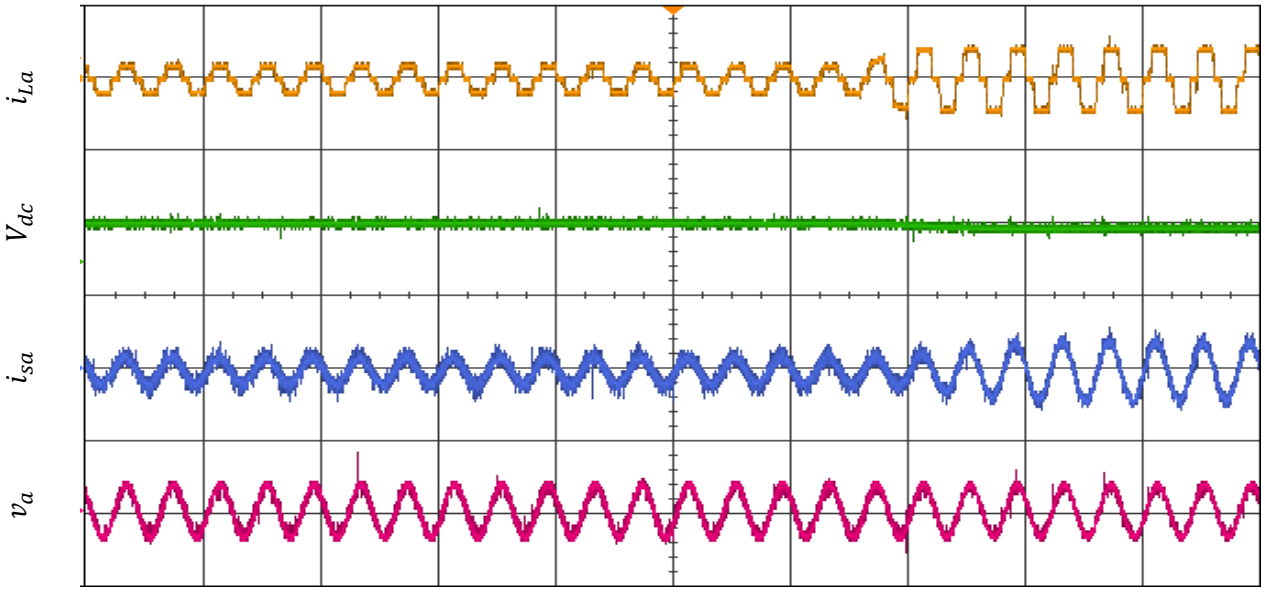

Fig 5.24 Experimental performance of DSTATCOM with CTF control and waveform of Load current (i_{La}), DC bus voltage (V_{dc}), Source current (i_{sa}) after compensation and PCC voltage (v_a)

Fig 5.25 shows compensation of source current using character of triangle based control algorithm in real time. THD of source current reduces to 3.2%.

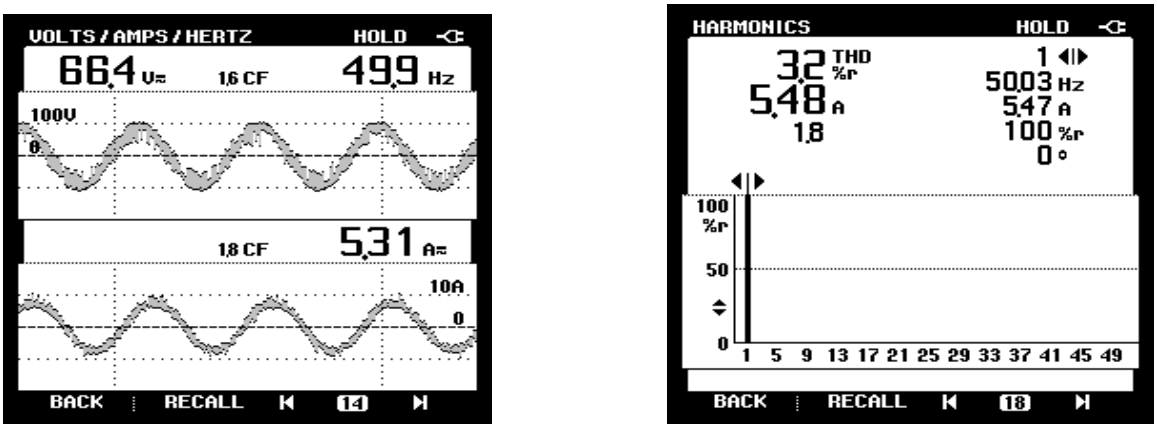

Fig 5.25 Source current after compensation and THD for same using CTF based control algorithm for DSTATCOM

5.3.4 MATLAB Simulation of Improved Linear Sinusoidal Tracer (ILST) based control algorithm

In adaptive theory based ILST technique, fundamental load current component is subtracted from load current. Error value of current passed through a band pass filter shown by Fig 5.26. This filtered value is added to output signal, this output is then multiplied by power frequency signal. Integration of this signal gives fundamental load current component of one phase.

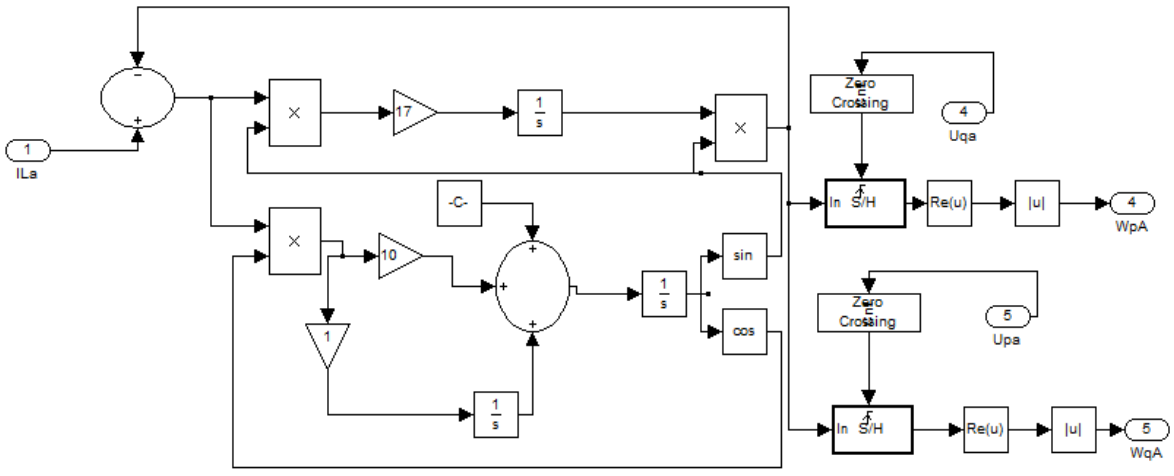

Fig 5.26 Reference current extraction using ILST for phase 'a'

To estimate active power component, zero crossing detector is used along with sample and hold circuit. Input to zero crossing detector is quadrature unit template for extraction of in-phase component of load fundamental current. Similar calculation is done for other phases.

5.3.4.1 Results and Discussions

ILST based control algorithm eliminates harmonics of source current. To determine the effectiveness of compensation provided by DSTATCOM, total harmonic distortion (THD) of source current is calculated using FFT window of MATLAB before compensation and after compensation.

(i) Simulation Results

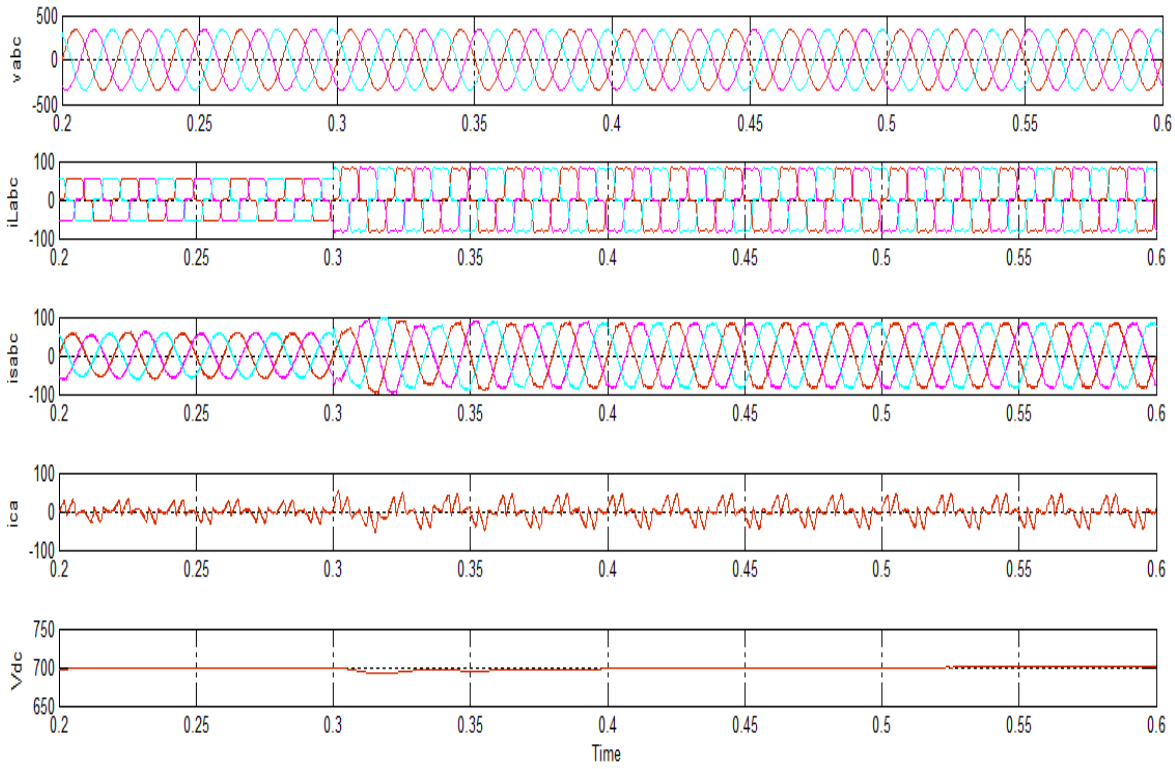

Fig 5.27 Performance of DSTATCOM with ILST controller while sudden switching of additional load at t=0.3sec and waveform of 3-phase line voltage (v_{abc}), 3-phase load current (i_{Labc}), 3-phase source current (i_{sabc}), Compensating current (i_{ca}) and DC link voltage (V_{dc}).

This scheme is also tested under the same load conditions. It is observed that using ILST the recovery in dip at DC capacitor voltage is faster. It is required in above 0.15sec. Also it does not introduce any significant time delay, as shown in Fig 5.27. In Fig 5.27, dynamic performance of DSTATCOM using ILST based current extractor is shown. At 0.3 sec of time load is increased suddenly (i.e. 32kVA from 16kVA). About 0.16 sec of time is elapsed to maintain DC Bus voltage again.This scheme has shown a considerable reduction in THD of source current. THD of source current is 3.10%, as shown in Fig 5.28 and apart from that THD of voltage is very low of about 0.26%.

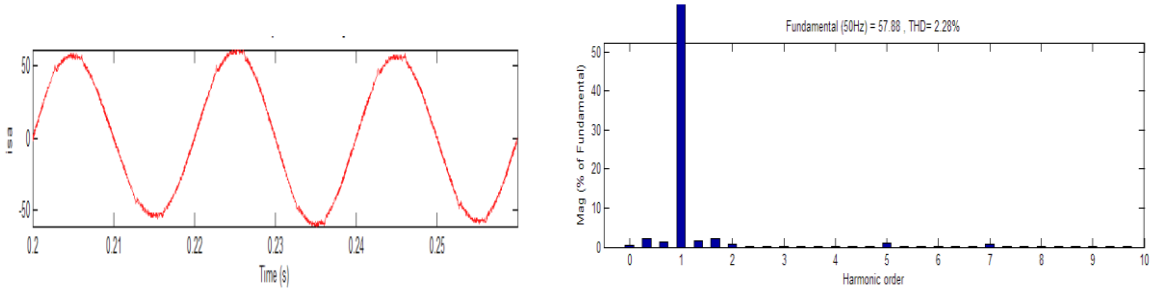

Fig 5.28 THD of source current using ILST

(ii) Experimental Results

ILST based control algorithm validated through experimental results. THD after compensation is only 3.6% in comparison of 27.3% as shown by uncompensated system.

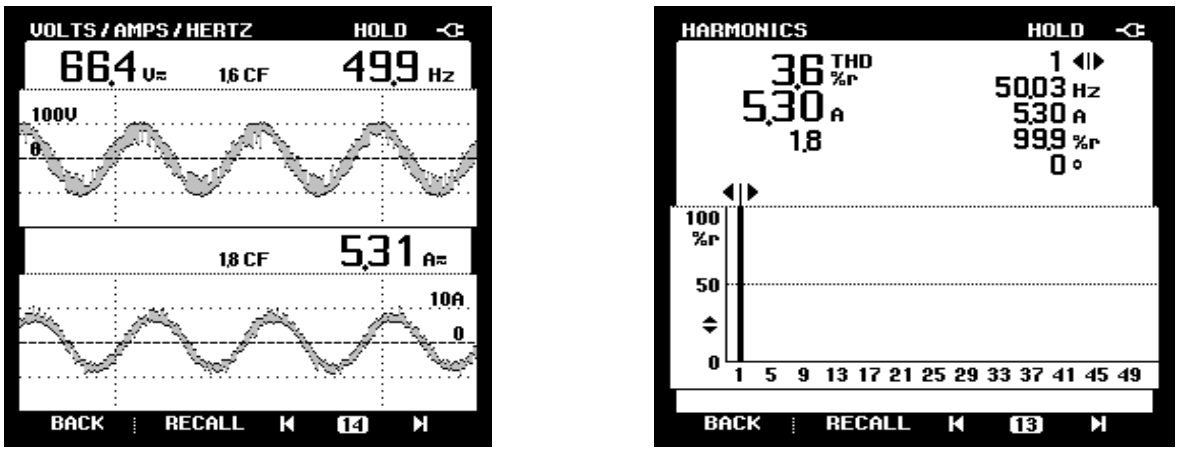

Fig 5.29 Source current after compensation and THD for same using ILST based control algorithm for DSTATCOM

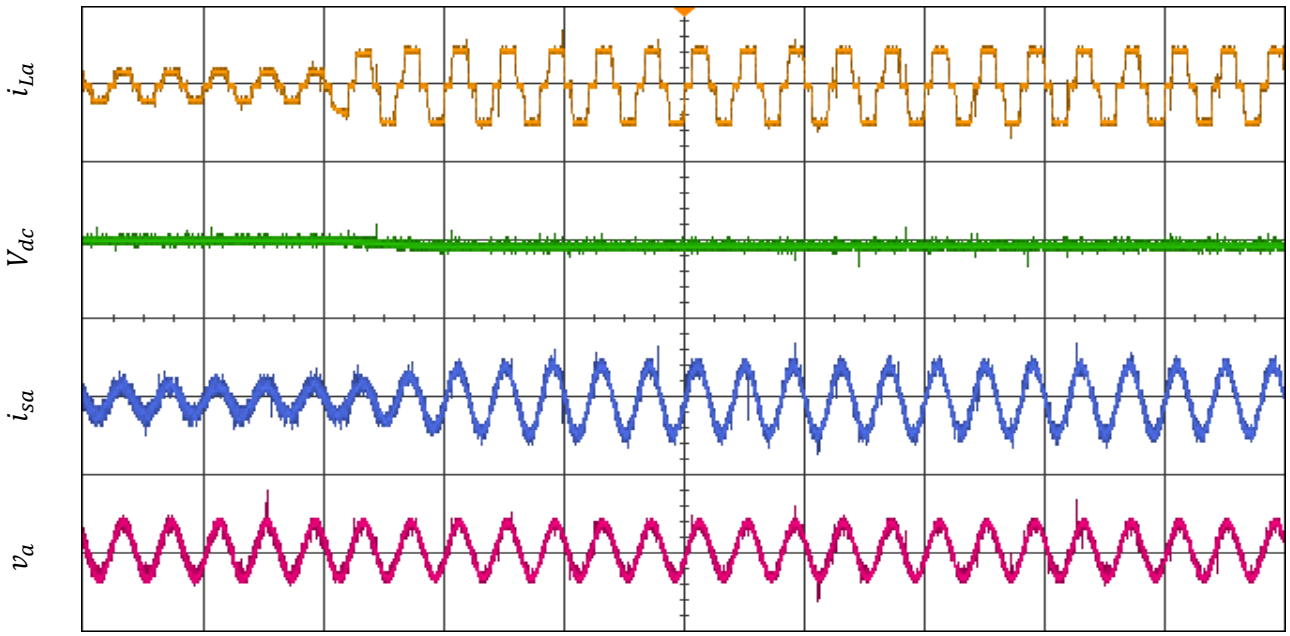

Fig 5.30 Experimental performance of DSTATCOM with ILST control and waveform of Load current (i_{La}), DC bus voltage (V_{dc}), Source current (i_{sa}) after compensation and PCC voltage (v_a)

Fig 5.30 shows behavior of system when load is suddenly changed in the system. In this figure, load current, dc bus voltage, source current after compensation and voltage at PCC as shown. This figure shows that source current changes from non sinusoidal nature to sinusoidal by providing compensation.

5.4 Performance Comparison of SRF, AH, CTF and ILST based control of DSTATCOM in a non-linear load

The two main dynamic performance parameters of DSTATCOM, THD in source current and time acquired to maintain DC bus voltage dip are compared for a DSTATCOM connected to three-phase ac supply feed a three-phase rectifier load.

5.4.1 Simulation Results

Table 1 shows a comparison of SRF, AH, CTF and ILST based control algorithms implemented in MATLAB SIMULINK. These algorithms are implemented on

same voltage level of 415V (L-L) and for same load of 16kVA. Comparison of algorithms is done on the basis of THD of source current for same load current THD of 23.6%. Other parameter of comparison is THD of source voltage. As shown in this table, THD in source current is almost same for both Anti-hebbian and ILST but time to maintain DC bus voltage is least for Anti-Hebbian. Hence Anti-hebbian is an effective and accurate method of harmonic elimination.

TABLE 1

S.NO.	**ALGORITHM**	THD (i_s)%	THD(v_s)%	THD(i_L)%	Tracking Speed (sec)
1.	SRF	3.38	0.17	23.6	0.2s
2.	ANTI-HEBBIAN	2.43	0.13	23.60	0.1s
3.	CTF	3.10	0.12	23.56	0.3s
4.	ILST	2.28	0.14	23.58	0.16s

5.4.2 Experimental Results

Table 2 shows a comparison of different control algorithms implemented on experimental setup.

TABLE 2

S.NO.	**ALGORITHM**	THD (i_s)%	THD(v_s)%	THD(i_L)%
1.	SRF	3.3	1.4	27.3
2.	ANTI-HEBBIAN	2.2	1.4	27.3
3.	CTF	3.2	1.4	27.3
4.	ILST	3.6	1.4	27.3

In this table control algorithms are compared on the basis of source current THD for same load current THD of 27.3%. As shown in this table, THD in source current is least for Anti-Hebbian. Hence both simulation and hardware results are same.

CHAPTER 6
MAIN CONCLUSIONS AND FUTURE SCOPE OF WORK

6.1 General

In this dissertation four control algorithms are implemented for operation of DSTATCOM to eliminate harmonics in source current due to non-linear load. MATLAB simulation model are designed for all four systems and simulated results are analyzed. Hardware model for the system are also developed to validate the simulated results.

6.2 Main Conclusion

In this dissertation work, four control algorithms synchronous reference frame (SRF) theory, Anti-Hebbian learning algorithm, character of triangle function (CTF) and improved linear sinusoidal tracer (ILST) are implemented and compared for harmonic elimination, power factor correction and tracking capability to maintain DC bus voltage. In these four algorithms, SRF is conventional. SRF algorithm has a disadvantage to produce some time lag in the system. This time delay is responsible for heavy circulating current in the system sometimes. Some of the new techniques based on artificial intelligence like Anti-Hebbian are able to reduce this time delay. Along with reducing the time lag, this algorithm also reduces the noise effect in the system. One more factor which decides the effectiveness of control algorithm is designing of algorithm. For designing of CTF, there is a need of only multipliers, comparators, etc. So its implementation is easy as compared to other techniques. ILST has good detection accuracy, adjustment of internal parameters is easy, stable performance and fast dynamic responses are main features. In this algorithm both frequency and time domain characteristics are not affected by external environment change.

6.3 Future scope of work

There are various further areas where these FACTS devices (STATCOM, BESS, SSSC) will find the application. Some of the areas of application are mentioned below

(i) Power quality improvement with BESS

(ii) Damping of SSR (sub synchronous resonance) using BESS.

(iii) Enhancement in GRID stability with BESS.

(iv) Improvement of distributed generation stability using BESS

REFERENCES

[1] N. G. Hingorani and L. Gyugyi, *Understanding FACTS: Concepts and Technology of Flexible AC Transmission Systems*. New York: IEEE Press, 2000.

[2] Arindam Ghosh, *Power Quality Enhancement using custom Power Devices*, Kluwer Academic Publishers.

[3] H. Akagi, E. H. Watanabe, and M. Aredes, Instantaneous Power Theory and Applications to Power conditioning, Hoboken, NJ: Wiley, 2007.

[4] K. K. Sen, "STATCOM—STATic synchronous COMPensator: Theory, modeling, and applications," in *Proc. IEEE Power Engineering Society Winter Meeting*, pp. 1177–1183, 1999.

[5] Dong Ju Lee , Eun Woong Lee, Jong Han Lee , Jong Gyeum Kim,*"Simulation of Static Synchronous Compensator (STATCOM)"*, pp. 1401-1403.

[6] Tariq Masood, R.K. Aggarwal, S.A. Qureshi, R.A.J Khan, "STATCOM Model against SVC Control Model Performance Analyses Technique by MATLAB", *International Conference on Renewable Energies and Power Quality*, Granada (Spain), 23rd to 25th March, 2010.

[7] Dong Shen, Wenhua Liu and Zhonghong Wang, "Study on the Operation Performance of STATCOM under Unbalanced and Distorted System Voltage", 0-7803-5935-6, IEEE, pp. 2630-2635, 2000.

[8] S. H. Hosseini and A. Ajami , "Transient stability enhancement of AC transmission system using STATCOM", *Proc. of IEEE TENCON02*, pp. 1809-1812, 2002.

[9] Wang Chao and Zhang Yao, "Approach on Nonlinear Control Theory for Designing STATCOM Controller", *Proceedings of 2007 IEEE International Conference on Grey Systems and Intelligent Services*, pp. 871-875, November 18-20, 2007, Nanjing, China.

[10] M. Tavakoli Bina, and Ashoka K. S. Bhat, "Averaging Technique for the Modeling of STATCOM and Active Filters", *IEEE transaction on power electronics*, vol. 23, no. 2, pp. 723-734, March 2008.

[11] Javid Akhtar, Sinto George, "Modeling and Simulation of STATCOM for a power system network using MATLAB/SIMULINK", *IOSR Journal of Engineering (IOSRJEN) ISSN: 2250-3021* vol. 2, no. 8, pp. 12-17, August 2012.

[12] Boon Teck Ooi, *Gem* boos and Xiaogang Huang, "Operating principles of shunt STATCOM based on 3-level diode-clamped converters", *IEEE Transaction3 on Power Delivery*, Vol. 14, No. 4, pp.1504-1510, October1999.

[13] Jianye Chen, Shan Song and Zanji Wang, "Analysis and Implement of Thyristor-based STATCOM", *International Conference on Power System Technology*, pp. 1-4, 2006.

[14] Bhim Singh, Kamal Al-Haddad and Ambrish Chandra, "A review of active filters for power quality improvement,*"IEEE Transactions on Industrial Electronics*, vol. 46, no. 5, pp. 960-971, October 1999.

[15] G. Casaravilla, F. Fnaiech, K. Al-Haddad and S. Rahmani," Adaptive linear combiners a robust neural network technique for on-line harmonic tracking," *Proc. of 34lb Annual Conference of IEEE Industrial Electronics*, pp. 530-534, 2008.

[16] Bhim Singh and Jitendra Solanki "A Comparison of Control Algorithms for DSTATCOM*", IEEE Trans. On Industrial electronics,* vol.56 no. 7, pp. 2738-2745, July 2009.

[17] D. M. Divan, S. Bhattacharya, and B. Banerjee, "Synchronous frame harmonic isolator using active series filter," in *Proc. Eur. Power Electron.Conf.*, 1991, pp. 3030–3035.

[18] Bhim Singh and Vishal Verma*, "*Selective Compensation of Power-Quality Problems Through Active Power Filter by Current Decomposition" , *IEEE transaction on power delivery*, vol. 23, no. 2, pp. 792-799, April 2008.

[19] G.-C. Hsieh and J. C. Hung, "Phase-locked loop techniques. A survey,"*IEEE Trans. Ind. Electron.*, vol. 43, no. 6, pp. 609–615, December 1996.

[20] B. Widrow, J. M. McCool, and M. Ball, "The complex LMS algorithm,"*Proc. IEEE*, vol. 63, no. 4, pp. 719–720, April 1975.

[21] Shaba Raj Arya, Bhimsingh, Ambrish Chandra and Kamal-Al Haddad, “Control of Shunt Custom Power Device Based on Anti-Hebbian Learning Algorithm”, 978-1-4673-2421-2/12 IEEE, pp. 1256-1261, 2012.

[22] S. Janpong, K. L. Areerak and K. N. Areerak,"A literature survey of neural network applications for shunt active power filters,"*Journal of World Academy of Science, Engineering and Technology*, vol. 60, pp. 392-398,2011.

[23] Liu Chuanlin and Liu Kaipei,"On instantaneous characteristic of adaptive harmonic detection based on LMS," *Proc. of Asia-Pacific Power and Energy Engineering Conference,* pp. 1-3, March 2010.

[24] Keqin Gao, M. Omair Ahmad and M. N. S. Swamy,"A constrained Anti-Hebbian learning algorithm for total least-squares estimation with applications to adaptive FIR and IIR filtering,*"IEEE Transactions on Circuits and Systems-II: Analog and Digital Signal Processing*, vol. 41,no. I, pp. 718-729, Nov 1994.

[25] Qun Wang, Ning Wu and Zhaoan Wang,"A neuron adaptive detecting approach of harmonic current for APF and its realization of analog circuit,*"IEEE Transactions on Instrumentation and Measurement*, vol. 50, no.1, pp.77-84, Feb.2001.

[26] Wang Xuhong and Xiao Jinhua,"RBF neural network based predictive of active power filter,*"Proc. of 1 Olh IEEE Region Conference TENCON,* vol. 4, pp. 109- 112, 2004.

[27] A. Zouidi, F. Fnaiech, K. Al-Haddad and S. Rahmani," Adaptive linear combiners a robust neural network technique for on-line harmonic tracking,*"Proc. of 34lb Annual Conference of IEEE Industrial Electronics*, pp. 530-534, 2008.

[28] A. Zouidi, F. Fnaiech, K. Al-Haddad and S. Rahmani,"Artificial Neural Networks as Harmonic Detectors,*" Proc. of 37'd Annual Conference on IEEE Industrial Electronics*, pp.2889-2892, 2006.

[29] Liu Chuanlin and Liu Kaipei,"On instantaneous characteristic of adaptive harmonic detection based on LMS," *Proc. of Asia-Pacific Power and Energy Engineering Conference*, pp. 1-3, March 2010.

[30] Mohsen Mojiri, Masoud Karimi-Ghartemani and Alireza Bakhshai, "Time-Domain Signal Analysis Using Adaptive Notch Filter", *IEEE Trans. On signal processing*, vol. 55, no.1, pp. 85-93, January 2007.

[31] Davood Yazdani, AlirezaBakhshai, GézaJoós and Mohsen Mojiri, "A Real-Time Extraction of Harmonic and Reactive Current in a Nonlinear Load for Grid-Connected Converters", *IEEE Transaction on industrial electronics*, vol. 56, no.6, pp. 2185-2189, June 2009.

[32] R. Bojoi, L. R. Limongi, D. Roiu , A. Tenconi, "Enhanced Power Quality Control Strategy for Single-Phase Inverters in Distributed Generation Systems", *IEEE Trans. on power electronics*, vol. 26, no. 3, pp. 798-806, March 2010.

[33] Zhihua Bao, Zongcheng Wang and Shibing Zhang, "A Predictive Deadbeat Control in Shunt Active Power Filter", in proc. of international conference on wireless communication and signal conditioning, pp.1-4, 2011.

[34] Sabha Raj Arya and Bhim Singh, "CTF control algorithm of DSTATCOM for Power factor correction and zero voltage regulation", *Sustainable Energy Technologies (ICSET), 2012 IEEE Third International Conference* , 10.1109/ICSET.2012.6357391 , pp. 157-162, 2012.

[35] S. Ali Khajehoddin, Masoud Karimi-Ghartemani, Praveen K. Jain, and Alireza Bakhshai, "A Control Design Approach for Three-Phase Grid-Connected Renewable Energy Resources", *IEEE Transaction on sustainable energy*, vol. 2, no. 4, pp. 423-432, October 2011.

[36] Bhim Singh and Sabha Raj Arya, "Adaptive Theory-Based Improved Linear Sinusoidal Tracer Control Algorithm for DSTATCOM", *IEEE Trans. on power electronics,* vol. 28, no. 8, pp. 1-8, August 2013.

[37] A. Chandra, B. Singh, B. N. Singh, and K. Al-Haddad, "An improved control algorithm of shunt active filter for voltage regulation, harmonic elimination, power-factor correction, and balancing of nonlinear loads, *IEEE Trans. Power Electron.*, vol. 15, no. 3, pp. 495–507, May 2000.

[38] V. George and M. K. Mishra, "Design and analysis of user-defined constant switching frequency current-control-based four-leg DSTATCOM," *IEEE Trans. Power Electron.*, vol. 24, no. 9, pp. 2148–2158, September 2009.

[39] S. Sharma and B. Singh, "Performance of voltage and frequency controller in isolated wind power generation for a three-phase four-wire system, "*IEEE Trans. Power Electron.*, vol. 26, no. 12, pp. 3443–3452, Dec. 2011.

[40] Y. F. Wang and Y. W. Li, "A grid fundamental and harmonic components detection method for single-phase systems," *IEEE Trans. Power Electron.*, vol. 28, no. 5, pp. 2204–2213, May 2013.

[41] European Patent Specification, EP 1 082 735 B1, 02.11.2006 Bulletin 2006/44.

[42] United States Patent, US 6317021 B1, 13.11.2001.

[43] United States Patent, US 2302893 B1, 24.11.1942.

[44] DS1104 R&D Controller Board, "Features", Release 7.3 – May 2012, www.dspace.com.

[45] DS1104 R&D Controller Board, "Hardware Installation and Configuration for DS1104 and CP1104/CLP1104 Connector Panels", Release 7.2 – November 2011.

[46] DS1104 R&D Controller Board, "RTI Reference", Release 7.3 – May 2012.

APPENDICES

Appendix A

Parameters for the Simulation and Hardware Setup

Fig 3.2 shows MATLAB based model of distribution system. This same model is designed in real time to validate the results of simulation with hardware. In simulation and hardware work three-phase ideal source of voltage 415V (L-L) and 110V (L-L) with resistance and inductance (R_s and L_s) as shown in table is used to provide power to the system. Considered load (R and L) value is shown below.

PARAMETERS	**SIMULATION**	**HARDWARE**
AC Line Voltage ,frequency	415V(L-L), 50Hz	110V(L-L),50Hz
Source impedance	Rs=0.06 Ω, Ls=3 mH	Rs=0.05Ω, Ls=1.1 mH
Load	R=20 Ω, L=200mH	R=10 Ω, L=80mH
Ripple Filter	R_f = 5 Ω, C_f = 7μf	R_f = 5 Ω, C_f = 6μf
DC bus Voltage	700V	200V
Interfacing inductor	L_f=2.3mH (SRF) L_f=2.1mH (AH) L_f=2.8mH (ILST) L_f=3.2mH (CTF)	L_f= 3mH (SRF) L_f= 2.9mH (AH) L_f=3.1mH (ILST) L_f=3.7mH (CTF)
Max Switching Freq	20kHz	20kHz

Appendix B

ALGORITHM	FOR DC BUS VOLTAGE	FOR PCC VOLTAGE
SRF	Kp= 1, Ki=0.01	Kp=0.03, Ki=0.03
Anti-Hebbian	Kp=0.8, Ki=0.1	Kp=0.1, Ki=0.001
CTF	Kp= 0.8, Ki=0.75	Kp=0.01, Ki=0.004
ILST	Kp=1, Ki=0.01	Kp=0.09, Ki=0.05

There are two PI controllers in the system. One is to maintain DC bus voltage and other is for maintain PCC voltage constant. Proportional and Integral gain constant (K_p and K_I) values are shown. Four control algorithms with different values are shown in above appendix.

Appendix C

DS-1104 technical specifications

Main Processor:
- MPC8240, PowerPC 603e core, 250 MHz
- 32 kByte internal cache

Timers:
- 1 sample rate timer, 32-bit down counter
- 4 general purpose timers, 32 bit
- 64-bit time base for time measurement

Memory:
- 32 MByte synchronous DRAM (SDRAM)
- 8 MByte boot flash for applications

Interrupt Control Unit:
- Interrupts by timers, serial interface, slave DSP, incremental encoders, ADC, host PC and 4 external inputs
- PWM synchronous interrupts

Analog Input:
- 4 ADC inputs, 16 bit, multiplexed
- ± 10 V input voltage range

	• 2μs sampling time
	• >80 dB signal-to-noise ratio
	• ADC channels, 12 bit
	• ± 10 V input voltage range
	• 800 ns sampling time
	• > 65 dB signal-to-noise ratio
Analog Output:	• 8 channels, 16 bit, 10 μs max. settling time
	• ± 10 V output voltage range
Incremental Encoder:	• Two digital inputs, TTL or RS422
Interface:	• 24-bit digital incremental encoders
	• Max. 1.65 MHz input frequency, i.e. four fold pulse counts up to 6.6 MHz
	• 5 V / 0.5 A sensor supply voltage
Digital I/O:	• 20-bit digital I/O (bit-selectable direction)
	• ± 5 mA output current
Serial Interface:	• Serial UART (RS232, RS485 and RS422)
Slave DSP Subsystem:	• Texas Instruments' DSP TMS320F240
	• 4 kWord of dual-port RAM
	• Three-phase PWM outputs plus 4 single PWM outputs
	• 14 bits of digital I/O (TTL)
Physical Characteristics:	• Power supply5 V, 2.5 A / -12 V, 0.2 A /12 V,0.3A
	• Requires one 32-bit PCI slot

Appendix D

ABB Voltage Sensor (EM010-9237)

V_{PN} = 200V

V_A = ±12 V…24 V

R_E = 10 K (input resistance)

R_M = 4.7 K (measuring resistance)

LEM Voltage Sensor (LV-25P)

I_{PN} = 10 mA (primary nominal current rms)

V_{PN} = 10….500V

K_N = 2500 : 1000 (conversion ratio)

Vc = ±12….±15V (supply voltage ±5%)

R_M = 100(Rmin)…350(Rmax)

ABB Current Sensor (ABB-25P)

I_{PN} = 25A (primary nominal current rms)

K_N = 2500 : 1000 (conversion ratio)

Vc = ±12….±15V (supply voltage ±5%)

R_M = 100(Rmin)…350(Rmax)

R_E = 10kΩ